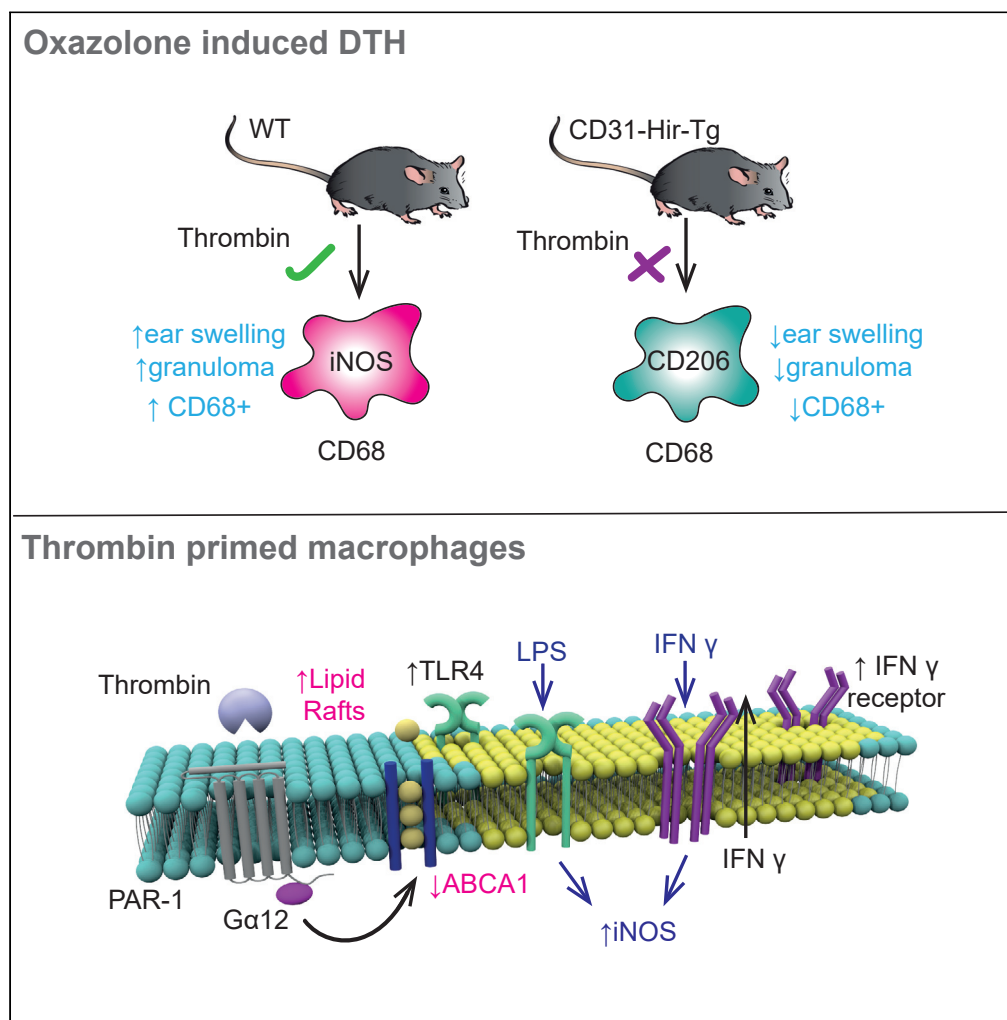


Article

PAR-1 signaling on macrophages is required for effective in vivo delayed-type hypersensitivity responses



Hannah Wilkinson, Hugh Leonard, Daxin Chen, ..., Pieter. Goossens, John H. McVey, Anthony Dorling

hannah.wilkinson@kcl.ac.uk (H.W.)
anthony.dorling@kcl.ac.uk (A.D.)

Highlights
Inhibiting thrombin signaling on monocytes is protective in type IV hypersensitivity

PTL060, a thrombin inhibitor, reduces inflammation in type IV hypersensitivity

Thrombin primes macrophages to be highly sensitive to IFN γ and LPS

Thrombin increases lipid rafts on macrophages in an ABCA1-dependent manner

Wilkinson et al., iScience 24, 101981
January 22, 2021 © 2020 The Author(s).
<https://doi.org/10.1016/j.isci.2020.101981>



Article

PAR-1 signaling on macrophages is required for effective *in vivo* delayed-type hypersensitivity responses

Hannah Wilkinson,^{1,5,*} Hugh Leonard,¹ Daxin Chen,¹ Toby Lawrence,² Michael Robson,¹ Pieter. Goossens,³ John H. McVey,⁴ and Anthony Dorling^{1,*}

Summary

Delayed-type hypersensitivity (DTH) responses underpin chronic inflammation. Using a model of oxazolone-induced dermatitis and a combination of transgenic mice, adoptive cell transfer, and selective agonists/antagonists against protease activated receptors, we show that PAR-1 signaling on macrophages by thrombin is required for effective granuloma formation. Using BM-derived macrophages (BMMs) *in vitro*, we show that thrombin signaling induced (a) downregulation of cell membrane reverse cholesterol transporter ABCA1 and (b) increased expression of IFN γ receptor and enhanced co-localization within increased areas of cholesterol-rich membrane microdomains. These two key phenotypic changes combined to make thrombin-primed BMMs sensitive to M1 polarization by 1000-fold less IFN γ , compared to resting BMMs. We confirm that changes in ABCA1 expression were directly responsible for the exquisite sensitivity to IFN γ *in vitro* and for the impact on granuloma formation *in vivo*. These data indicate that PAR-1 signaling plays a hitherto unrecognized and critical role in DTH responses.

Introduction

Macrophages are heterogeneous and versatile cells found in virtually all tissues of adult mammals. Activation of macrophages has emerged as a key area of immunology, tissue homeostasis, disease pathogenesis, and resolving and non-resolving inflammation. Early literature described them dichotomously as M1 or M2 macrophages (Mills, 2015), with M1 macrophages being the classical inflammatory macrophages induced by T-cell-dependent (interferon γ [IFN γ]) and T-cell-independent (lipopolysaccharide [LPS]) pathways. These promote upregulation of Th1 proinflammatory chemokines and cytokines such as IL-6, IL-12, and IL-23. They upregulate HLA-DR, thus having a role in antigen presentation and induce nitric oxide production. In contrast to M1 macrophages, M2 macrophages are anti-inflammatory having roles in tissue homeostasis and repair and have roles in the Th2 response. M2 macrophages are classically induced by IL-4 or IL-13. As time has progressed, these two are recognized as extreme phenotypes, with subtypes described *in vivo* appearing more plastic and often expressing characteristics of both. Subsets with a predominant M2 phenotype (M2a-d) have been defined, having anti-inflammatory roles in the Th2 response (M2a), suppression of tumor growth (M2b), immune regulation and tissue remodeling (M2c), and angiogenesis (M2d). These M2 subsets have different polarizing stimuli, eg. IL-4/13 – M2a, immune complexes, and toll-like receptor (TLR) ligands – M2b, IL-10 & TGF- β – M2c and IL-6 for M2d macrophages. Further subsets have been defined in the field of atherosclerosis research (Adamson and Leitinger, 2011) including further anti-inflammatory atheroprotective subtypes M(Hb) M(heam) and Mox (Moore et al., 2013). What is becoming clear is the classical/alternative model of macrophage activation does not take into account the subtle changes occurring in the cell microenvironment which can have tangible changes to the cell phenotype without fully polarizing the cells.

Type IV or delayed-type hypersensitivity (DTH) is the archetypal antigen-specific cell-mediated immune response involving CD4⁺ T cells and monocytes/macrophages. In the sensitization phase, antigen-presenting cells present the hapten (e.g., oxazolone) to naive T cells. The T cells then expand to a group of hapten-specific T-helper1 (TH1) cells. In the effector phase, re-challenge with the same hapten leads to

¹Department of Inflammation Biology, School of Immunology & Microbial Sciences, King's College London, Guy's Hospital, London SE1 9RT, UK

²Centre for Inflammation Biology and Cancer Immunology, School of Immunology & Microbial Sciences, King's College London, London SE1 9RT, UK

³Department of Pathology, Cardiovascular Research Institute Maastricht (CARIM), Maastricht University, 6229HX Maastricht, the Netherlands

⁴School of Bioscience & Medicine, Faculty of Health and Medical Sciences, University of Surrey, Guildford GU2 7XH, UK

⁵Lead contact

*Correspondence: hannah.wilkinson@kcl.ac.uk (H.W.), anthony.dorling@kcl.ac.uk (A.D.)

<https://doi.org/10.1016/j.isci.2020.101981>



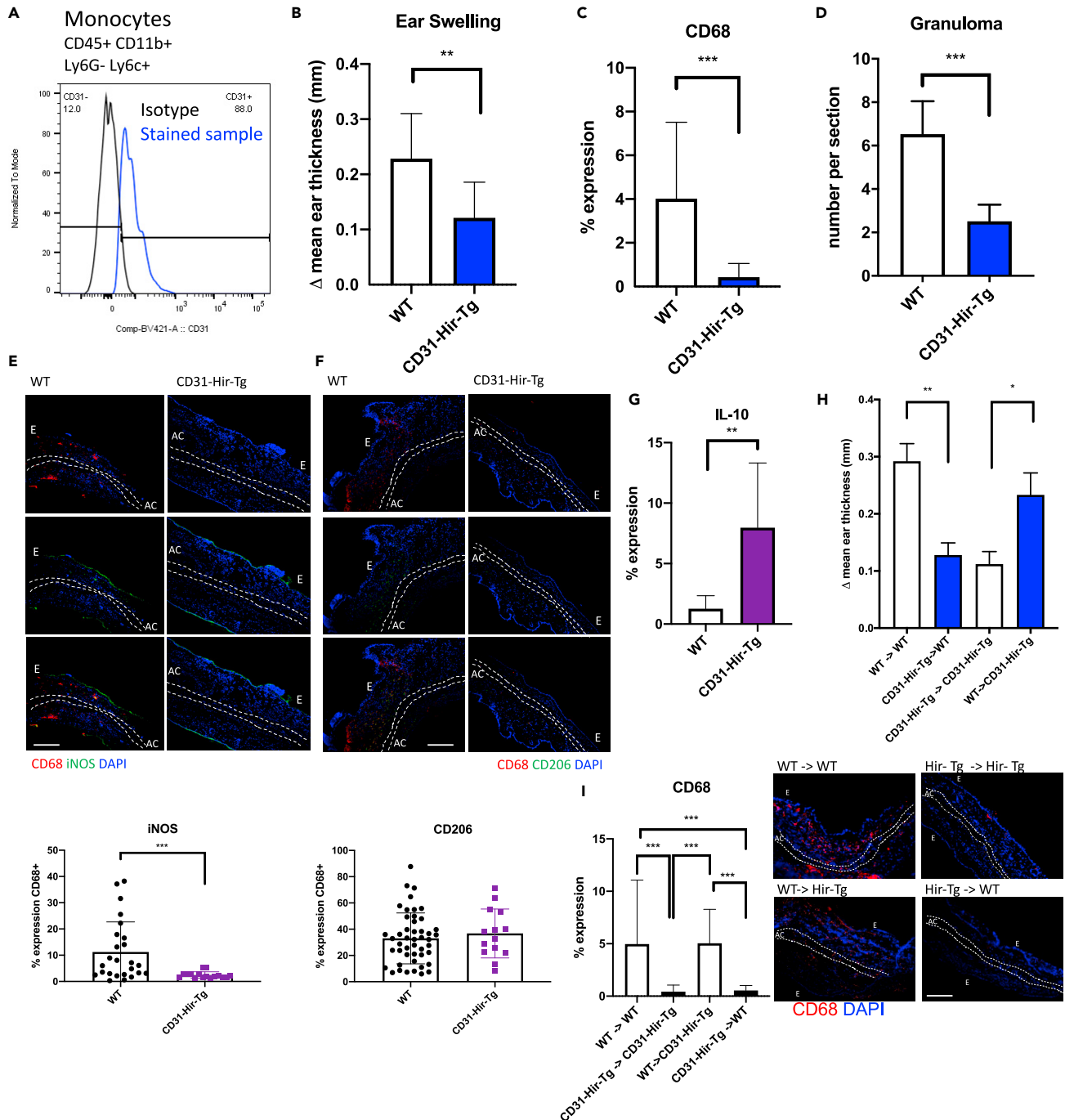


Figure 1. Results of oxazolone-induced delayed-type hypersensitivity experiments in transgenic mice

(A) Surface CD31 expression on monocytes (as defined as CD45 + CD11b + Ly6G- Ly6c+) on the peripheral blood of CD31-Hir-Tg mice.
 (B) Difference in ES at 24 hr. This is derived by subtracting thickness of the right ear (oxazolone) from that of the left (control) ear. WT group n = 6, transgenic group n = 6.
 (C) Immunofluorescence (IF) analysis of CD68 expression with the ear. Expression calculated by % lesion area occupied by CD68 + cells.
 (D) Granuloma assessed as the average number per section at 100X magnification. A granuloma was defined as a collection of CD68+/CD3+ cells outpouching from the epidermis.
 (E–G) IF analysis of proportion of CD68 + cells expressing iNOS (E), CD206 (F), or IL-10 (G). Graphs show percentage of CD68 cells that co-stain with iNOS or CD206 or in the case of IL-10, the % lesional area occupied by IL-10 + cells. Representative images show the following: CD68, red; CD206 or iNOS, green; DAPI, blue. The scale bar shows 200 μ m in distance.

Figure 1. Continued

(H) Bone marrow chimeric mice underwent oxazolone-induced DTH: graph shows change in ES at 24 hr compared to vehicle control ear. WT recipients of WT bone marrow and CD31-Hir-Tg recipients of CD31-Hir-Tg bone marrow represent experimental controls. Group numbers WT (CD45.1) -> WT (CD45.1) n = 3, CD31-Hir-Tg -> WT (CD45.1) n = 6, CD31-Hir-Tg -> CD31-Hir-Tg n = 6, WT (CD45.1) -> CD31-Hir-Tg n = 6.

(I) IF results of macrophage infiltration (CD68, red; DAPI, blue) within the ear of the bone marrow chimeric mice. Associated graph shows expression calculated by % lesion area taken up by CD68 + cells when corrected for background fluorescence. The scale bar shows 200 μ m in distance. Data are represented as mean \pm standard error of mean (SEM). *P \leq 0.05, **P \leq 0.01, ***P \leq 0.001, ****P \leq 0.0001. E = epidermis, AC = auricular cartilage.

rapid expansion of the of the sensitized TH1 cells which then interact with resting macrophages leading to macrophage activation via IFN γ and tumor necrosis factor beta (TGF- β) (Chen et al., 2019). These interactions underpin the chronic inflammatory lesions characteristic of inflammatory bowel disease, chronic infection, sarcoidosis, and rejection of transplanted kidneys (Black, 1999).

Thrombin is a serine protease generated at the site of tissue injury and is the main effector enzyme in the coagulation cascade (Coughlin, 2005; Shrivastava et al., 2013). Thrombin generation is initiated by tissue factor (TF), a transmembrane protein found on the adventitia of vessels, as well as on tissue macrophages, dendritic cells, and at low levels on circulating monocytes. In addition to the well-described role of thrombin in coagulation, it has a direct effect on a wide array of cell types such as smooth muscle cells, platelets, and endothelial cells (ECs) (Cunningham et al., 2000). These cellular responses of thrombin are mediated through a family of G-protein-coupled protease activated receptors (PARs), designated PAR-1-4 (Coughlin, 2005). PARs are characterized by an activation mechanism whereby proteolytic cleavage at specific sites within the extracellular amino-terminus leads to the exposure of an amino-terminal "tethered ligand" domain. This new amino terminus is then able to affect transmembrane signaling (Vu et al., 1991). Thrombin is able to cleave PAR-1,-3, and -4 but not PAR-2 (Cunningham et al., 2000). TF, factor Xa, factor VIIa, trypsin, and mast cell tryptase, among others, are able to signal through PAR-2 (Camerer et al., 2000). While there is a wealth of data exploring the role of thrombin as an inflammatory mediator, there is yet to be a robust description of how thrombin acts on innate immune cells. This prompted us to investigate how thrombin signaling in monocyte/macrophages impacts the DTH response. We show that thrombin signaling through PAR-1 signaling plays a hitherto unrecognized and critical role in DTH responses, inducing downregulation of cell membrane reverse cholesterol transporter ATP-binding cassette transporter 1 (ABCA1) and increased expression of IFN γ receptor. These two key phenotypic changes combined to make thrombin-primed bone-marrow-derived macrophages extremely sensitive to M1 polarization.

Results**Inhibition of thrombin on CD31 + myeloid cells inhibits DTH responses to oxazolone**

In order to investigate the role of thrombin in DTH responses, we induced a DTH response in the ear skin in response to oxazolone in either C57BL/6 wild-type (WT) or CD31-Hir-Tg mice. CD31-Hir-Tg mice express a fusion protein containing the direct thrombin inhibitor hirudin on all CD31 + cells including all circulating monocytes (Figure 1A) (Chen et al., 2004a). CD31-Hir-Tg mice had significantly reduced ear swelling (ES) compared to WT at 24 (p = 0.0019) and 48 (p = 0.0024) hours after re-challenge with oxazolone (Figure 1B). Immunofluorescence analysis of the ear sections revealed a reduction in the total number of macrophages as assessed by reduced CD68 + expression within the ear lesion from 4.9% in WT to 0.5% in CD31-Hir-Tg (p < 0.001) (Figure 1C), a reduction in the number of granulomas per section (Figure 1D) and a shift in the phenotype of recruited cells to a more anti-inflammatory profile with significantly reduced ratio of iNOS:CD206 expression on CD68 + cells coupled with an increase in IL-10 expression (Figures 1E-1G).

As the transgenic fusion protein in CD31-Hir-Tg mice is expressed on all CD31 + cells, we generated bone marrow (BM) chimeras with WT (CD45.1) mice to isolate expression on either BM-derived elements (platelets and monocytes) (Chen et al., 2004a) or ECs alone. Cells expressing CD45.1 allele (WT) can be distinguished from cells expressing the CD45.2 allele (CD31-Hir-Tg), allowing the easy tracking of donor and host leukocytes. Engraftment at day 30 was >95%. CD45.1 mouse recipients of CD31-Hir-Tg BM had a similar ES phenotype to parental CD31-Hir-Tg mice (Figure 1H), whereas CD31-Hir-Tg recipients of CD45.1 BM had a WT phenotype. Similarly, CD68 expression within the ear was reduced in the CD45.1 recipients of transgenic (CD-31-Hir-Tg) BM in comparison to CD31-Hir-Tg recipients of CD45.1 BM (Figure 1I).

There was a reduced T-cell (CD3+) infiltration into the ears of the CD31-Hir-Tg mice but no difference in IFN γ expression within the lesion (Figure 2A). To assess whether the expression of the transgenic fusion

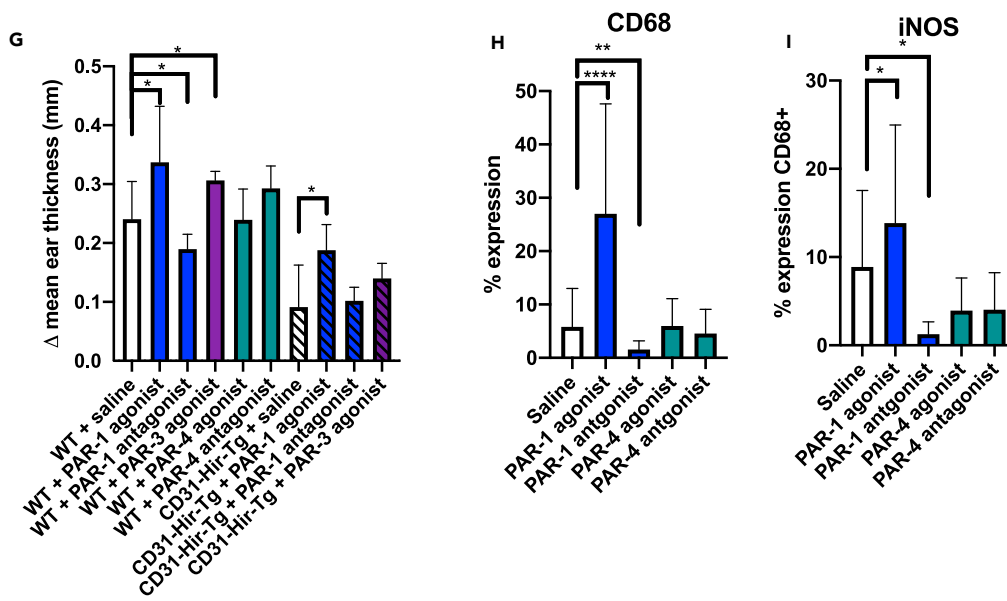
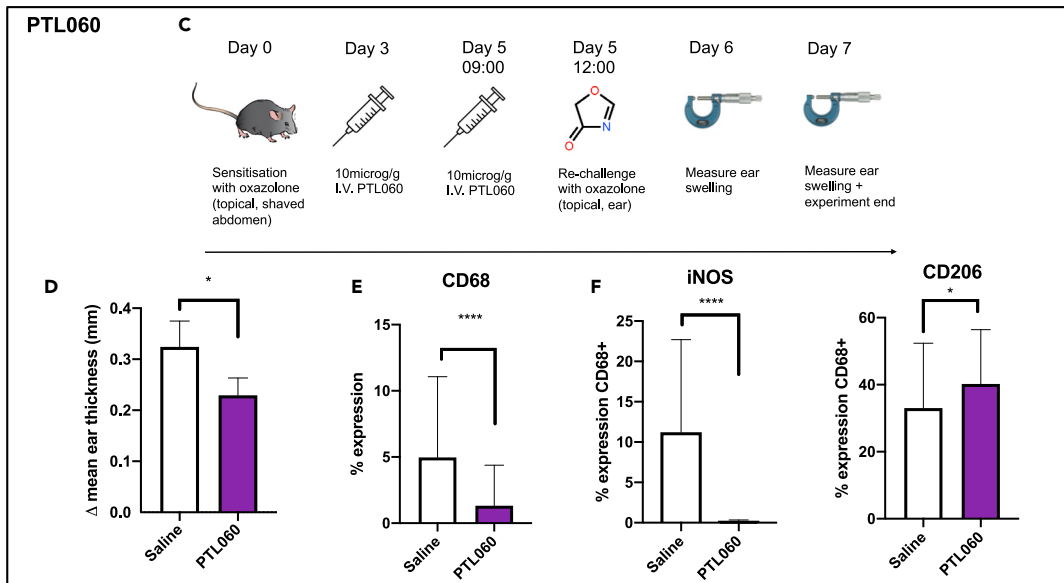
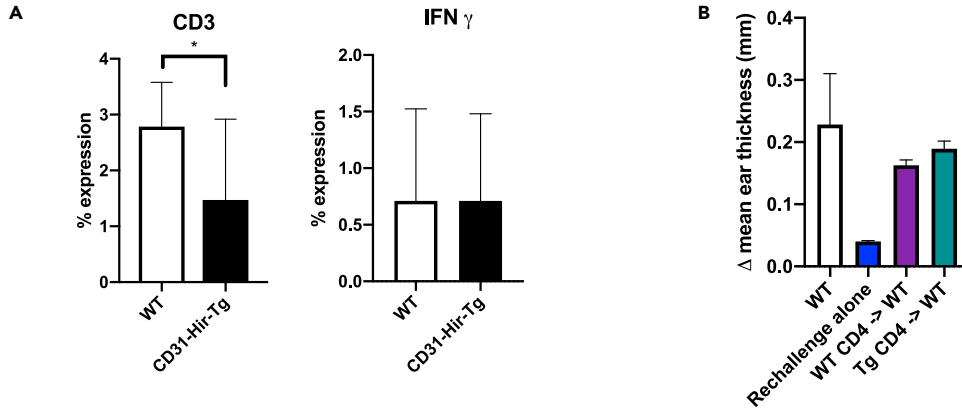


Figure 2. Assessing how transgenic expression of hirudin influences T-cell priming in type IV hypersensitivity and evaluating role of PAR signaling

(A) CD3 and IFN γ expression in the WT or CD31-Hir-Tg mice after DTH. CD3 or IFN γ expression calculated by % lesion area taken up by CD3+ or IFN γ cells when corrected for background. WT group n = 6, transgenic group n = 6.

(B) Adoptive transfer of oxazolone primed WT or CD31-Hir-Tg CD4 cells into WT mice before oxazolone applied to the ear. Change in ear thickness, compared to vehicle challenge alone, was measured at 24 hr. WT control mice received IV saline instead of cells but abdominal oxazolone challenge on day 0 and then ear re-challenge on day 5. "Re-challenge alone" mice were oxazolone-naive mice that received only 1% oxazolone in acetone and olive oil to the right ear. WT group n = 6, re-challenge alone n = 2, WT CD4 - > WT n = 4, Tg CD4 - > WT n = 6.

(C) PTL060 experimental protocol.

(D) ES results of WT (C57BL/6) mice treated with IV 10mcg/g PTL060 (n = 6) or equivalent volume saline (n = 4) on day 3 and 5 after sensitization in oxazolone-induced DTH model.

(E) IF analysis of CD68 expression within the ear of PTL060-treated group vs saline.

(F) IF analysis of iNOS and CD206 expression on CD68 + cells in the PTL060-treated group vs saline.

(G) The effect of PAR signaling on DTH responses. Before a re-challenge on day 5, WT or CD31-Hir-tg mice received 10 microM/g intraperitoneal (IP) PAR-1 agonist (TFLLR-NH2) (n = 5) or antagonist (RWJ 56110) (n = 5) or PAR-4 agonist (GYPGQV trifluoroacetate salt) (n = 5) or antagonist (tcY-NH2) (n = 4) or PAR-3 agonist (H-Ser-Phe-Asn-Gly-Gly-Pro-NH2) (n = 5). The ears were then painted with oxazolone or vehicle alone. Data represent change in ES at 24 hr compared to the control ear.

(H) IF analysis of CD68 expression within WT ears. Expression calculated by % lesion area taken up by CD68 + cells when corrected for background.

(I) IF analysis of iNOS expression on CD68 + cells in WT ears. Data are represented as mean \pm standard error of mean (SEM). *P \leq 0.05, **P \leq 0.01, ***P \leq 0.001, ****P \leq 0.0001.

protein influenced T-cell priming, CD4+ T cells were isolated from the spleens of CD31-Hir-Tg or WT mice 5 days after initial exposure to oxazolone. These sensitized CD4+ T cells were then injected via the tail vein into oxazolone-naive WT mice who then underwent the usual re-challenge step with oxazolone. Recipients of CD31-Hir-Tg CD4 T cells had similar degrees of ES as recipients of WT controls (Figure 2B), indicating that CD4+ T-cell priming in CD31-Hir-Tg mice was "normal" and suggesting that the protective effect of the transgenic fusion protein was due to its expression on monocytes. There was no difference in circulating coagulation parameters: D-dimers, fibrinogen, thrombin antithrombin complex, TF, or thrombin activity between the WT and CD31-Hir-Tg mice (Figure S1), suggesting there was no systemic activation of coagulation proteases nor consumption of fibrinogen. However, the inflammation in control ears was accompanied by widespread local fibrin deposits, which were significantly diminished and appeared to be located predominantly only subepithelial in the oxazolone-treated ears of CD31-Hir-Tg mice, suggesting that the DTH response did involve local activation of coagulation proteases (Figure S2).

PTL060 is a cytotoxic thrombin inhibitor based on Hirulog. On IV injection, a microstyl tail anchors it into the lipid bilayer of circulating monocytes (and other cells) (Chen et al., 2020). When C57BL/6 mice undergoing DTH were treated with 10 μ g/g IV PTL060 on day 3 and day 5 (3 hr before re-challenge) (Figure 2C), there was a reduction in ES compared to saline control (p = 0.0121) (Figure 2D). Examination of the ears by immunohistochemistry revealed, in comparison to saline controls, PTL060 lead to a reduction in CD68 infiltration from 4.9% to 1.3% (p < 0.0001) (Figure 2E) and the adoption of a more anti-inflammatory profile with an increase in CD68 + cells expressing CD206 33%–40% (p = 0.0332) and completely inhibited iNOS expression on CD68 + cells (11%–0% < 0.0001) (Figure 2F).

We postulated that the transgenic fusion protein was most likely influencing the phenotype by blocking thrombin activation of PAR-1. Therefore, prior to re-challenge, mice were treated with intraperitoneal PAR-1 agonists or antagonists. WT mice treated with a PAR-1 agonist (TFLLR-NH2) had an increase in ES (p = 0.0279), CD68 expression (p < 0.0001) with increased iNOS expression (p = 0.0212) when compared to saline controls (Figures 2G, 2H, and 2I), whereas those treated with a PAR-1 antagonist (RWJ 56110) had reduced ES (p = 0.0322), CD68 expression (0.0036), iNOS expression (p = 0.0104) compared to saline controls (Figure 2G, 2H, and 2I). (Experiments using different PAR-1 agonists and antagonists yielded entirely consistent results [data not shown].) Treatment with PAR-4 agonist (GYPGQV trifluoroacetate salt) or antagonist (tcY-NH2) had no impact on the outcome of DTH. Although a PAR-3 agonist (H-Ser-Phe-Asn-Gly-Gly-Pro-NH2) increased ES in WT mice (Figure 2G), it did not significantly increase ES in CD31-Hir-Tg mice, whereas those treated with a PAR-1 agonist developed significantly increased ES (p = 0.0219) (Figure 2G), suggesting that only the provision of a PAR-1 signal on CD31-Hir-Tg cells was sufficient to overcome the effect of thrombin inhibition.

All these data suggest that local generation of thrombin at the site of antigen re-challenge leads to activation of PAR-1 that critically contributes to the development of the recall response; inhibition of thrombin

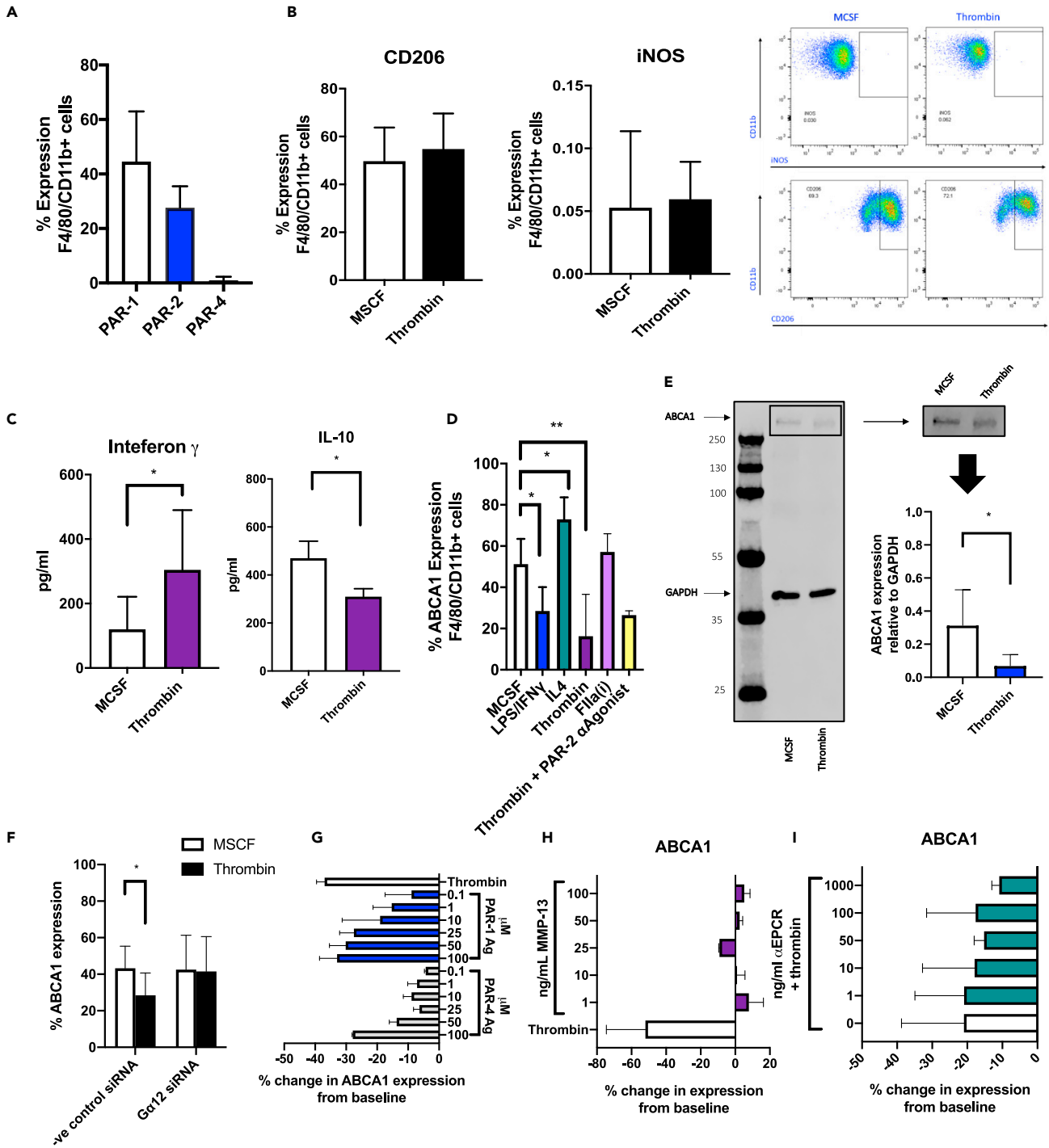


Figure 3. Thrombin induces a proinflammatory state without fully polarizing the cultured macrophages and downregulates ABCA1 expression through PAR-1

(A) Surface expression of PAR-1, -2, and -4 on bone marrow macrophages cultured for 5 days in complete bone marrow medium analyzed by flow cytometry. (B) Intracellular flow cytometric analysis of CD206 or iNOS expression on bone marrow macrophages cultured for 5 days in complete bone marrow medium and stimulated for 24 hr with 25 ng/ml MCSF or 50 units/ml of thrombin. Representative flow cytometry profiles are shown to the right.

(C) Cell culture supernatants taken from cells treated for 24 hr with 25 ng/ml MCSF or 50 units/ml thrombin were analyzed by ELISA. IFN γ ELISA n = 5, IL-10 ELISA n = 4. *P \leq 0.05.

Figure 3. Continued

(D) ABCA1 expression, analyzed by flow cytometry, on F4/80 CD11b-positive cells after 5 days in bone marrow culture followed by 24 hr stimulation with 25 ng/ml MCSF, 100 ng/ml LPS, and 50 ng/ml IFN γ for M1 cells and 25 ng/ml IL4 for M2 cells or 50 units/ml thrombin or equimolar active site inhibited thrombin (Fllai) or the PAR-2 antagonist (PAR-2 α agonist) FSLLRV-NH2 for 2 hr prior to thrombin stimulation. Data are taken from at least 4 experiments. (E) Western blot of MCSF or thrombin-treated cells. Representative gel is shown to the right. ABCA1 band confirmed at approx. 250 kDa. (F) Surface ABCA1 expression of cells transfected with siRNA to G α 12 or negative control siRNA for 24 hr and then thrombin or MCSF for 24 hr. Data analyzed by flow cytometry. Data are taken from 3 experiments. (G) ABCA1 expression, analyzed by flow cytometry, on F4/80 CD11b-positive cells after 5 days in bone marrow culture followed by 24 hr stimulation with 25 ng/ml MCSF, thrombin, or increasing amounts of TFLLRV-NH2 (PAR-1 agonist peptide) or GYPGQV trifluoroacetate salt (PAR-4 agonist peptide). Data represent percentage change in expression from control (MCSF) stimulated cells. (H and I) Change in surface ABCA1 expression analyzed by flow cytometry of bone marrow macrophages cultured for 24 hr with MMP-13 (H) or precultured for 2 hr with a neutralizing ePCR antibody prior to thrombin stimulation (I). Data shown as percentage change from baseline expression of MCSF media maintained cells in 3 different experiments. Data are represented as mean \pm standard error of mean (SEM). *P \leq 0.05, **P \leq 0.01, ***P \leq 0.001, ****P \leq 0.0001.

on monocytes/macrophages either through transgenic expression of hirudin or local tethering of hirulog significantly inhibits the DTH.

Macrophage responses to thrombin

To assess how thrombin signaling influences the behavior of WT macrophages, BM isolates were incubated with 25 ng/ml macrophage colony-stimulating factor (MCSF) for 5 days, which was found to be the time at which PAR-1 expression was maximal (Figure 3A). Cells were then stimulated for a further 24 hr with either thrombin or maintained in MCSF alone as a control. There was no change in iNOS or CD206 expression compared to baseline in response to thrombin (Figure 3B). Enzyme-linked immunosorbent assay (ELISA) confirmed a significant increase in IFN γ concentration in cell culture supernatants from thrombin-stimulated cells compared to controls (304.6 pg/ml vs 119.9pg/ml, respectively p = 0.0185), as well as a significant reduction in IL-10 production (454pg/ml vs. 309pg/ml p = 0.0286) (Figure 3C).

ABCA1 plays a critical role in lipid homeostasis and orchestrates the principal cellular pathway leading to cholesterol efflux (Pradel et al., 2009). We found that ABCA1 expression was highest in MCSF-matured BM cells that were treated with IL-4 for 24 hr and lowest after culture for 24 hr with a combination of LPS and IFN γ (Figure 3D). This is in keeping with previously published data (Singaraja et al., 2002). Next, we evaluated what role thrombin had on ABCA1 expression. Thrombin, but not active site-inhibited thrombin, down-regulated surface ABCA1 expression by flow cytometric analysis from 51.27% to 16.28% after 24 hr culture (p = 0.0024) (Figure 3D). Thrombin-mediated reduction in ABCA1 was also seen on Western blot (p = 0.0303) (Figure 3E). This was shown to be reliant on the G protein subunit G α 12 as inhibiting this with small interfering RNA (siRNA) prevented thrombin-mediated ABCA1 downregulation (Figure 3F). Thrombin-cleaved PAR-1 is known to transactivate PAR-2 (O'Brien et al., 2000). Blocking the PAR-2 signal with the PAR-2 antagonist FSLLRV-NH2 prior to thrombin stimulation did not affect the outcome of thrombin on ABCA1 expression (Figure 3D). This thrombin-mediated ABCA1 downregulation was mimicked by culturing cells with the PAR-1 agonist peptide (TFLLRV-NH2) (Figure 3G) and inhibited by antagonizing signaling through PAR-1 (Figure S3). Only at very high dose did PAR-4 agonist peptide (GYPGQV trifluoroacetate salt) impact ABCA1 expression (Figure 3G), whereas a PAR-3 agonist (H-Ser-Phe-Asn-Gly-Gly-Pro-NH2) failed to influence ABCA1 expression (Figure S4). Delivery of a signal through matrix metalloproteinase (MMP) 13 did not affect ABCA1 expression (Figure 3H). Noncanonical PAR-1 signaling can occur through the endothelial protein C receptor (ePCR) (Zhao et al., 2014). Preculturing the cells with an ePCR neutralizing antibody did not affect thrombin's ability to reduce ABCA1 expression (Figure 3I).

ABCA1 has been linked to the formation of lipid-rich microdomains in the external leaflet of the plasma membrane (Zhu et al., 2010). These discrete lipid domains, representing organized accumulations of cholesterol and glycosphingolipids, play a key role in inflammatory signaling due to the high concentration of cell receptors residing within the "lipid rafts" (Pike, 2003). To evaluate the role thrombin signaling had on lipid rafts, bone marrow derived macrophages (BMM) were incubated for 24 hr in complete media with MCSF or thrombin. After 24 hr, cells were stained using Vybrant Alexa Fluor 488 Lipid Raft Labeling Kit. The thrombin-treated cells had increased expression of cholera toxin B (CTB) on the cell surface, correlating with increased lipid raft formation (p < 0.0001) (Figure 4A). Surface expression of TLR4 increased

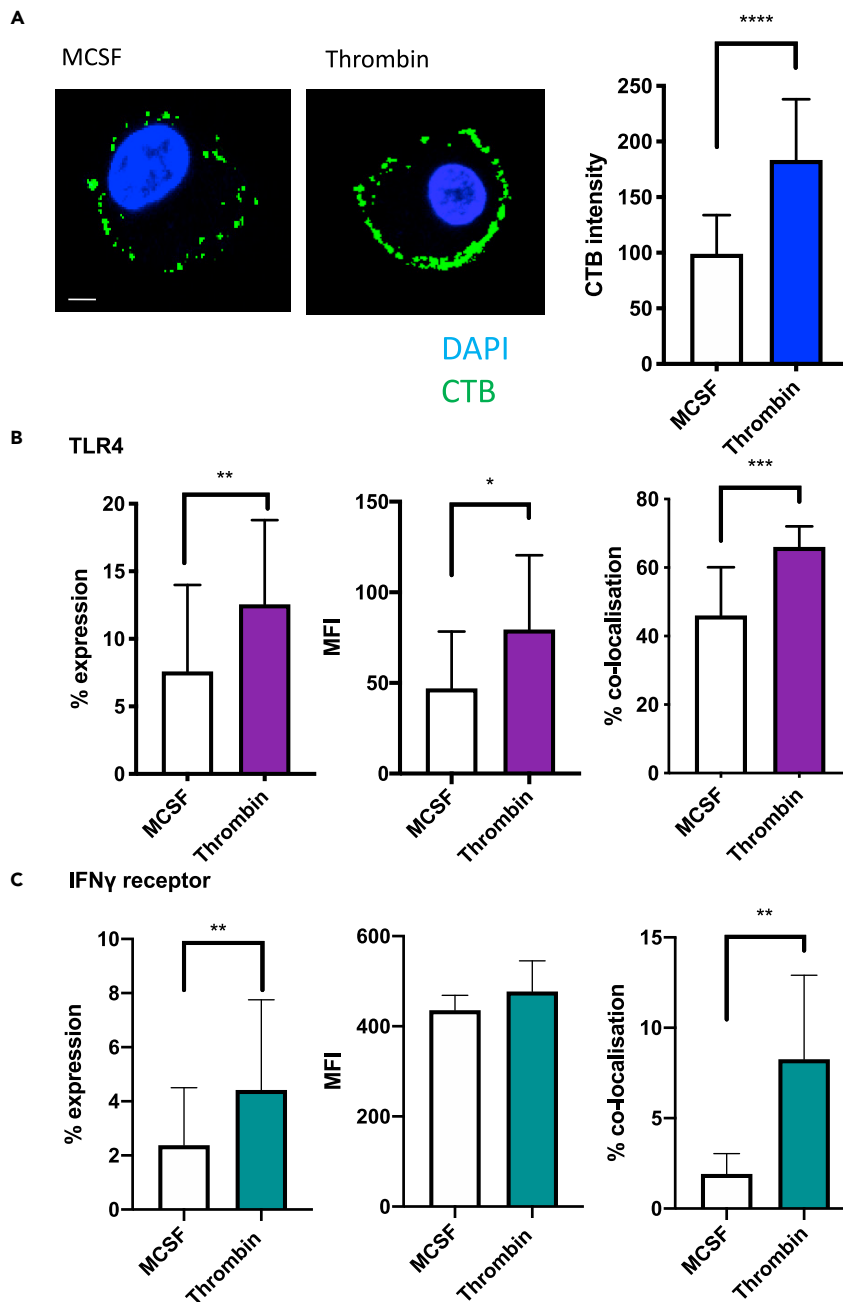


Figure 4. Thrombin increases the lipid raft content of cells

(A) CTB (green) or DAPI (blue) staining of MCSF and thrombin-treated cells. The scale bar shows 10 μ m in distance.

Associated graph shows graphical representation of CTB intensity.

(B) TLR4 surface expression as measured by IF on MCSF or thrombin-treated cells. Cells were prepared for lipid raft CTB staining as above and co-stained with fluorochrome-conjugated anti-TLR4 ab. The graphs represent, from left to right, the % of cells in positive gate, MFI of TLR4 on cells in the positive gate, and proportion of cells showing co-localization of CTB with TLR4. Costaining calculated using ICY cell imaging software using Pearson correlation coefficient of both CTB staining and TLR4 receptor staining.

(C) IFN γ surface expression as measured by IF on MCSF or thrombin-treated cells. Cells were prepared for lipid raft CTB staining as above and co-stained with fluorochrome-conjugated anti-IFN γ ab. The graphs represent, from left to right, the % of cells in positive gate, MFI of IFN γ on cells in the positive gate, and proportion of cells showing co-localization of CTB with IFN γ . Costaining calculated using ICY cell imaging software using Pearson correlation coefficient of both CTB staining and IFN γ receptor staining. Data are shown from 4 separate experiments. Data are represented as mean \pm standard error of mean (SEM). *P \leq 0.05, **P \leq 0.01, ***P \leq 0.001, ****P \leq 0.0001.

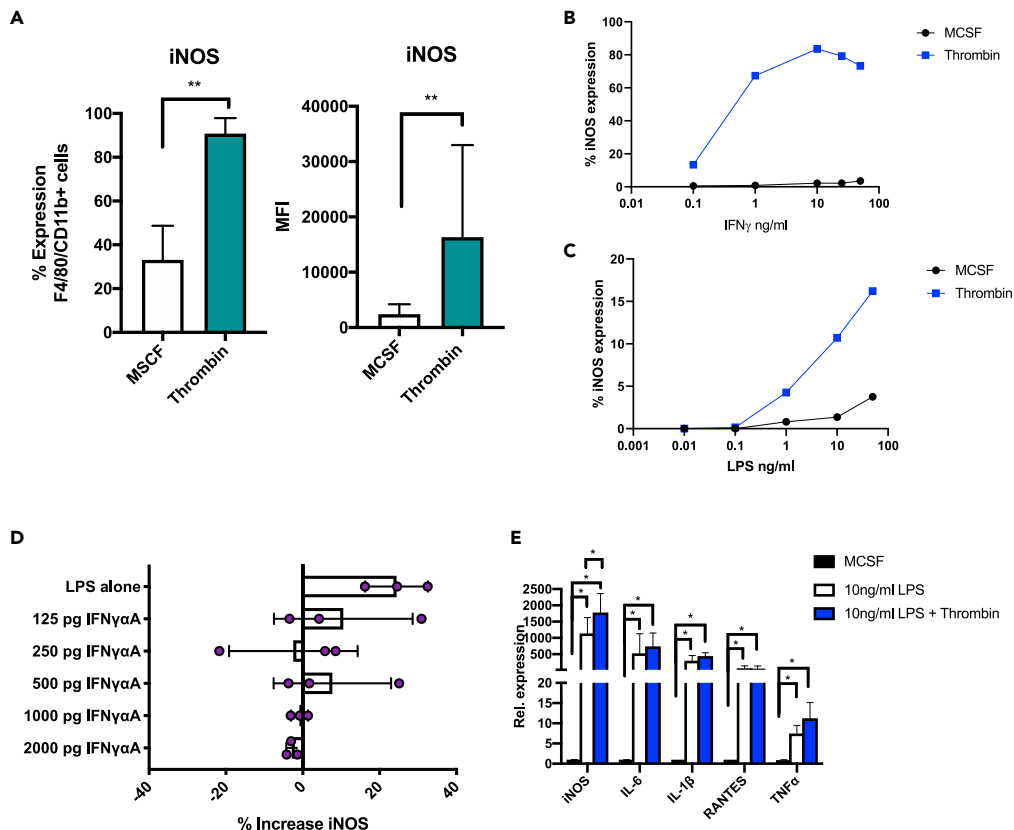


Figure 5. Priming with thrombin increases sensitivity to low-dose LPS and IFN γ

(A) Intracellular flow cytometric analysis of % of iNOS⁺ cells and MFI of iNOS expression by cells in the positive gate. Cells were murine bone marrow macrophages primed for 24 hr with thrombin or control (MCSF) $n = 6$ prior to 24-hr stimulation with low-dose M1 stimuli 0.01 ng/mL LPS and 50 ng/mL IFN γ $n = 6$.

(B and C) BMMs were primed for 24 hr with MCSF or 50 units/ml thrombin as indicated and then stimulated for a further 24 hr with escalating amounts of either IFN γ alone (B) or LPS alone (C). Cells were then analyzed by intracellular flow cytometry for iNOS expression. Data represent % positive cells.

(D) The effect of IFN γ blockade on heightened sensitivity to LPS alone. BMMs were cultured for 5 days with 25 ng/ml MCSF and then stimulated for 24 hr with thrombin. Media was replaced with fresh media containing escalating doses of IFN γ blocker (IFN γ Ag) (Abcam) for 1 hr. All wells were then treated with low-dose LPS (10 ng/ml) +/- thrombin for 24 hr. iNOS expression was then analyzed by flow cytometry. Data shown change in iNOS expression between control and thrombin-treated cells. Each data point represents a single experiment; bars represent mean of data.

(E) qPCR data for the expression of TNF α , IL-1 β , IL-6, RANTES, and iNOS. BMMs were stimulated for 24 hr with thrombin or maintained in complete media. After 24 hr, the media was removed and replaced with fresh media containing 10 ng/ml LPS +/- thrombin. Cells were removed for qPCR analysis 4 hr later. Data shown relative to MCSF control cells. Data are shown from 4 separate experiments. Error bars are means of data. Data are represented as mean \pm standard error of mean (SEM). * $P \leq 0.05$, ** $P \leq 0.01$, *** $P \leq 0.001$, **** $P \leq 0.0001$.

upon thrombin stimulation (mean fluorescence intensity [MFI] increased from 47.01 to 79.02 [$p = 0.0427$]), and there was also increased colocalization of the receptor within the lipid rafts (46.04% vs. 66.03% $p = 0.0004$) (Figure 4B). Thrombin stimulation increased surface expression of IFN γ receptor (MFI 435.6 vs 477.4) ($p = 0.0287$), and these also showed increased expression within the lipid rafts from 2.39% expression to 8.73% ($p = 0.0031$) (Figure 4C).

Thrombin primes BM-derived macrophages to be hyperresponsive to M1 polarizing signals

Given thrombin's apparent role in augmentation of lipid raft composition, specifically with the increase in both the LPS and IFN γ receptor—both moderators of the M1 phenotype—we considered that thrombin was priming the cells which could potentially translate to increased responsiveness to LPS or IFN γ . For

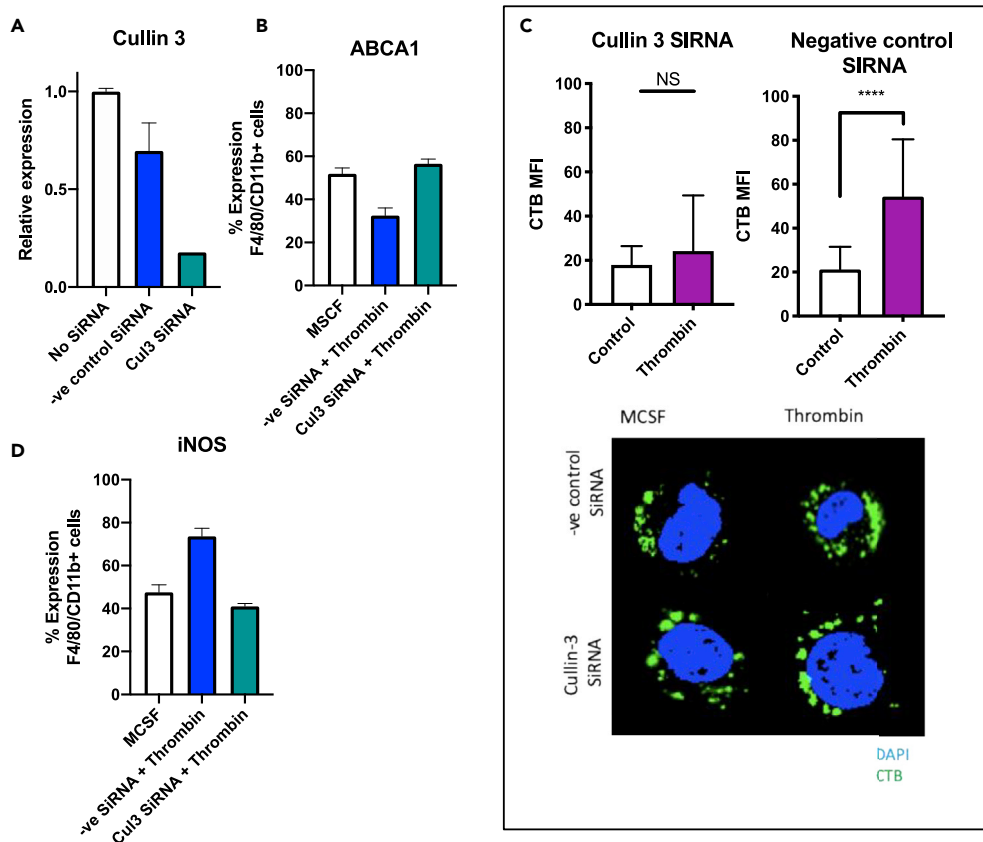


Figure 6. ABCA1 is essential for heightened sensitivity of thrombin-primed cells to LPS and IFN γ

(A) Cullin 3 expression, analyzed by qPCR, after 24 hr transfection of BMM cultured for 24 hr with cullin 3 siRNA, negative control siRNA, or control cells maintained in complete media containing 25 ng/ml MCSF.

(B) The above cells were then stimulated for 24 hr with thrombin, and surface ABCA1 expression was assessed by flow cytometry.

(C) CTB staining of lipid rafts of the three experimental cell groups after 24 hr siRNA (or control) transfection and then 24 hr of thrombin. Cells were counterstained with DAPI, then analyzed using an inverted confocal microscope at 60 \times magnification (oil immersion), and analyzed using NIS-Elements software. The scale bar shows 10 μ m in distance.

(D) The cells were then treated for a further 4 hr with 0.01 ng/ml LPS and 50 ng/ml IFN γ with or without thrombin and then analyzed by flow cytometry for intracellular iNOS expression. Data are shown from 3 different experiments. Data are represented as mean \pm standard error of mean (SEM). *P \leq 0.05, **P \leq 0.01, ***P \leq 0.001, ****P \leq 0.0001.

these experiments, BMM were incubated for 24 hr with thrombin or MCSF alone as a control followed by increasing concentrations of LPS and/or IFN γ . Thrombin-stimulated cells were more sensitive to the combination of low dose LPS/IFN γ , evidenced by increased proportion of iNOS expression (29.1% vs 89.3% p = 0.0079) and increased MFI (1543 vs. 9096 p = 0.0040) (Figure 5A). Thrombin-stimulated cells were exquisitely sensitive to very low dose IFN γ (in the absence of LPS) with increasing concentrations resulting in enhanced iNOS expression in a dose-dependent manner (Figure 5B). Similarly, but to a lesser extent, the cells were also sensitive to low-dose LPS (without IFN γ) (Figure 5C). These enhanced responses to low-dose LPS appeared to be due entirely to thrombin-mediated increases in IFN γ secretion, as they were abolished by increasing amounts of an IFN γ blocking antibody (Figure 5D).

LPS stimulation of the BMM increased the expression of iNOS (p = 0.0286), TNF α (p = 0.0030), RANTES (p = 0.0079), IL-6 (p = 0.0286), and IL-1 β (p = 0.0287) by qPCR. Pre-treatment with thrombin increased further iNOS expression (p = 0.0286) during LPS stimulation, but this heightened sensitivity to LPS was not seen in TNF α , RANTES, IL-6, or IL-1 β expression (Figure 5E). LPS and PAR-2 have been shown to synergistically enhance inflammatory signaling (Ostrowska et al., 2007). There was no difference in PAR-2 expression during thrombin stimulation, so the enhanced responses to low-dose LPS cannot be attributed to increased PAR-2 expression (Figure S5).

Thrombin-mediated downregulation of ABCA1 has been described to be via upregulation of the ubiquitin-proteasome system component cullin 3 (Raghavan et al., 2018). To assess the importance of ABCA1 to thrombin-mediated heightened sensitivity to low-dose M1 stimuli, cullin 3 siRNA was used to maintain ABCA1 expression (Figures 6A, 6B, and S6) in the face of thrombin stimulation. This inhibition of thrombin-mediated ABCA1 downregulation by cullin 3 siRNA was associated with a failure to increase cell membrane lipid rafts (Figure 6C) and a loss of the hypersensitivity to low-dose LPS/IFN γ seen after exposure to thrombin (Figure 6D).

Taken together, all these data indicate that thrombin, through PAR-1 signaling, primes BMM to polarization by IFN γ and TLR4 agonists. This is via an increase in expression of IFN γ , IFN γ receptor and TLR4, and co-localization of both receptors in membrane lipid-rich microdomains, due to the associated downregulation of ABCA1 by cullin 3.

ABCA1 is critical to the phenotype of ES in delayed-type hypersensitivity

To confirm that these mechanistic steps were operational in the DTH responses *in vivo*, we confirmed that CD31-Hir-Tg mice showed increased ABCA1 expression compared to WT mice (Figure 7A) after second exposure to oxazolone. BM isolates from CD31-Hir-Tg were not sensitive to thrombin and thus maintained ABCA1 expression in the face of thrombin (Figure 7B). Finally, CD31-Hir-Tg mice were treated with IP probucol for 3 days prior to oxazolone re-challenge (Figure 7C). Probucol inhibits ABCA1-mediated cellular lipid efflux but does not affect ABCA1 surface expression (Favari et al., 2004). The probucol-treated CD31-Hir-Tg mice had an increase in ES at 24 and 48 hr compared to saline-treated control CD31-Hir-Tg mice (Figure 7D), associated with increased infiltration by CD68 + cells (Figure 7E), expressing reduced levels of CD206 but increased levels of iNOS (without any change in ABCA1 expression) (Figure 7F).

Discussion

In this study, we describe how the serine protease thrombin is able to prime macrophages to become exquisitely responsive to low doses of LPS and IFN γ . We confirm the reports of others (Chinetti-Gbaguidi et al., 2015) that ABCA1 is a marker of IL-4 stimulated anti-inflammatory macrophages. Moreover, we describe the link between thrombin stimulation, lipid raft composition alteration, and increased sensitivity to M1 stimuli. Finally, to our knowledge, we provide the first report of ABCA1's key role in the development of normal DTH responses and the first report that thrombin-mediated PAR-1 signaling provides the stimulus *in vivo* for ABCA1 downregulation.

Thrombin is the main effector protein in the coagulation cascade (Manabe et al., 2009) but is able to directly affect a wide array of cell types such as smooth muscle cells, platelets, and ECs (Cunningham et al., 2000) via signaling through PARs. We have previously described the roles that thrombin plays in acute and chronic vascular inflammation using CD31-Hir-Tg mice (Chen et al., 2006, 2008a, 2008b). In a mouse-to-rat model of heart transplantation, hearts from CD31-Hir-Tg mice rejected significantly later compared to WT hearts (Chen et al., 2004b), due to inhibition of both intravascular thrombosis associated with antibody-mediated rejection (AMR) and inhibition of thrombin-dependent CCL2 chemokine gradients necessary for monocyte recruitment (Chen et al., 2006, 2008b) in this model. Aortas from these mice, when transplanted into apolipoprotein E (ApoE) $^{-/-}$ mice fed a high-fat diet, fail to express CCL2 and MIF and do not develop atherosclerosis, in contrast to the florid lesions seen in control WT aortas (Chen et al., 2020). Recently, we have reported pretransplant perfusion into rat or primate organs with PTL060 (or related compounds) prevents the intravascular thrombosis associated with AMR (Manook et al., 2017; Karegli et al., 2017). Most recently, we have showed that intravenous delivery of PTL060 into ApoE $^{-/-}$ mice fed a high-fat diet leads to widespread coating of the endothelium, inhibits expression of both CCL2 and MIF, and prevents atheroma formation (Chen et al., 2020). Importantly, in this work, intravenous delivery of PTL060 also led to widespread uptake onto the membranes of circulating leukocytes and was associated with significant regression of atherosclerotic plaques when treatment was started 16 weeks after the beginning of the high-fat diet (Chen et al., 2020). In this model, the direct effect of PTL060 on monocytes was the dominant mechanism driving atheroma regression, as the same phenotype was achieved by adoptive transfer of PTL060-coated monocytes.

The data in a contact dermatitis model, presented here, are entirely consistent with our data in atherosclerosis but provide a much greater mechanistic insight into the role and importance of thrombin in monocyte/macrophage polarization *in vivo*. Expression of a hirudin fusion protein on monocytes

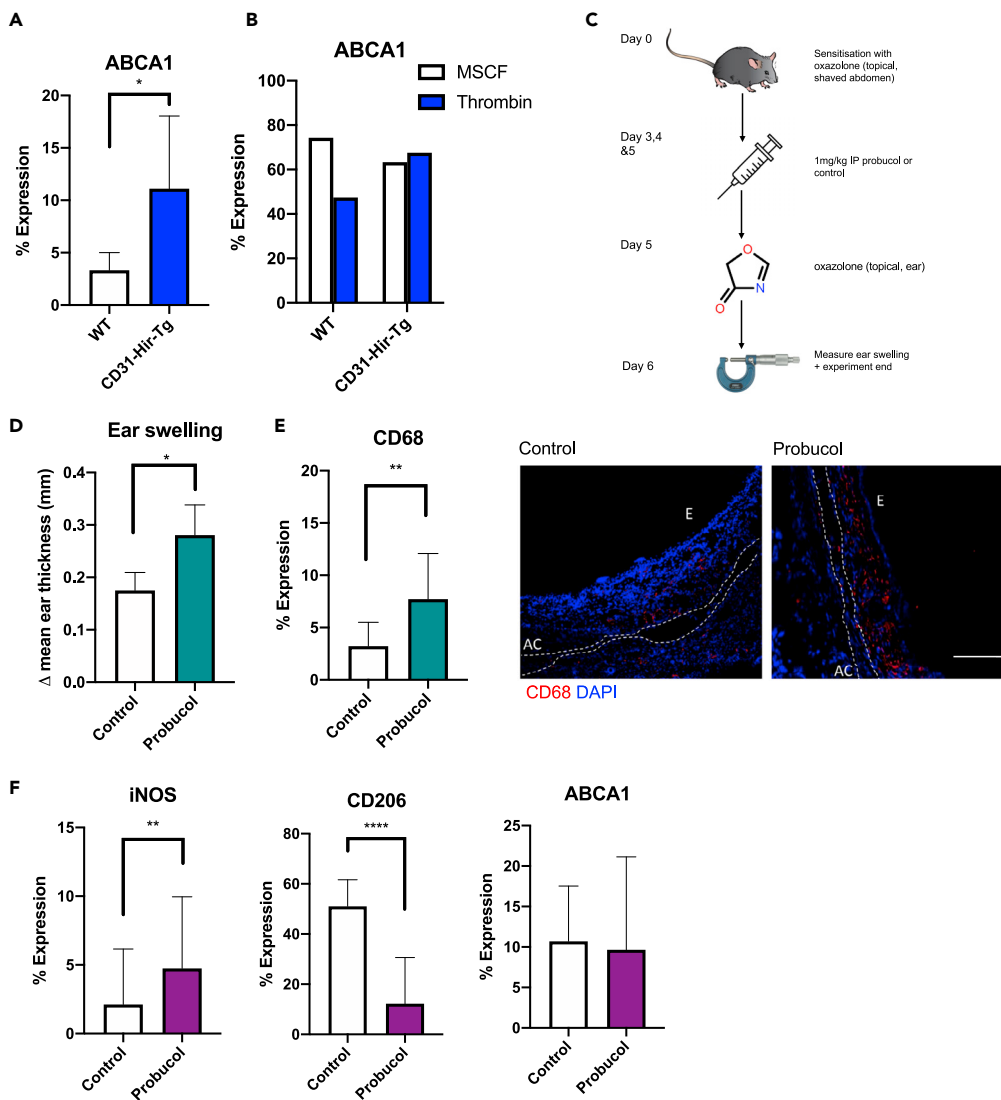


Figure 7. The importance of ABCA1 in vivo

(A) ABCA1 expression in the ears of WT or CD31-Hir-Tg mice after oxazolone-induced DTH measured by IHC. Represented as % of CD68 + cells co-expressing ABCA1. WT group n = 6, transgenic group n = 6.

(B) Flow cytometric analysis of surface ABCA1 expression of cultured WT or CD31-Hir-Tg BMM treated with 24 hr 50U/ml thrombin or MCSF control.

(C) IP probucol experiments. CD31-Hir-Tg mice were challenged with 5% oxazolone on day 0. Then, from day 2–5, they received 1 mg/kg IP probucol (n = 4) or control (n = 4) before re-challenge with oxazolone on day 5.

(D) Data represent difference in ES at 24 hr

(E) IP probucol experiments. IF analysis of CD68 expression with the ear. Expression calculated by % lesion area taken up by CD68 + cells when corrected for background. Representative images show the following: CD68, red; DAPI, blue. E = epidermis, AC = auricular cartilage. The scale bar shows 200 μ m in distance.

(F) IP probucol experiments. IF analysis of CD206, iNOS, and ABCA1 expression on CD68 + cells. Data are represented as mean \pm standard error of mean (SEM). *P \leq 0.05, **P \leq 0.01, ***P \leq 0.001, ****P \leq 0.0001.

prevented ES after second exposure to oxazolone and shifted the phenotype of DTH lesions away from an M1 spectrum toward M2. This was PAR-1 and ABCA1 dependent. Furthermore, we have demonstrated that PTL060 also delivers a protective phenotype in this additional model system.

Our *in vitro* experiments revealed the mechanistic basis of these findings. Thrombin, via PAR-1-mediated ABCA1 downregulation, increased the expression of IFN γ R and shifted the receptors into cholesterol-rich

microdomains, resulting in a massively increased sensitivity to IFN γ -mediated polarization. At the same time, TLR4 expression was increased within the same lipid rafts, and thrombin induced secretion of picomolar concentrations of IFN γ , which in combination, enhanced the sensitivity of cells to LPS-mediated polarization. Thrombin's nuanced role in LPS stimulation was further highlighted when pre-treatment with thrombin changed the expression of some (iNOS) but not all Myd88 and TRIF-dependent genes during TLR4 stimulation (Leifer and Medvedev, 2016). *In vitro* there appeared to be a correlation between high dose PAR-4 stimulation and ABCA1 expression. This is not entirely surprising as it is well documented that the PAR-4 receptor lacks the hirudin-like domain; therefore, higher concentrations of thrombin are required to initiate cellular signaling (Xu et al., 1998). We did not see any evidence of PAR-4 signaling affecting the outcome of the *in vivo* findings. In contrast, a PAR-3 agonist even at high doses failed to impact on ABCA1 expression, and although the same agent caused increase ES in WT mice, it did not partially reverse the phenotype of the CD31-Hir-Tg mice in the same way as a PAR-1 agonist, suggesting a minor role, if any for PAR-3 in this model. That said, a definitive conclusion about the role of PAR-3 is difficult in the absence of reliable reagents to antagonize PAR-3 activation.

We believe that, in this model, the thrombin is generated on the surface of myeloid cells, which are known to express TF (Rao and Pendurthi, 2012). We were able to demonstrate evidence of local fibrin generation in the WT mice but not the transgenic strain. Interestingly, there was no evidence of systemic activation of coagulation.

Other groups have previously reported on the impact of PAR-1 signaling on monocyte/macrophage function. In RAW cells, thrombin has been shown to induce iNOS (Kang et al., 2003). In human THP1 cells, thrombin has been linked to IL-8 production (Kang et al., 2003). In a model of *Citrobacter rodentium*-induced colitis, PAR-1 signaling on monocytes was shown to be key to promoting Th17-type immune response via IL-23 (Saeed et al., 2017). PAR-1 signaling has been shown to enhance the Poly I:C induction of the antiviral response via TLR3 in bone marrow macrophages (Antoniak et al., 2017). Recently, López-Zambrano et al. reported that thrombin signaling, in part through PAR-1, was sufficient to induce M1 polarization in bone marrow macrophages (Lopez-Zambrano et al., 2020). The difference between our data and this work is likely to be due to the use of L929 conditioned medium to differentiate the BMM instead of purified MCSF. Taken together, our data are consistent with the underlying implication that thrombin primes monocytes to make enhanced responses to microenvironmental polarization cues. Priming of monocytes has been described by others. Askenase et al. have recently described how monocytes are primed for regulatory function prior to egress from the bone marrow using a model of gastrointestinal infection. In this model, natural killer cell-derived IFN γ promoted regulatory programming in monocyte progenitors controlled by systemic IL-12 produced by Batf3-dependent dendritic cells in the mucosa-associated lymphoid tissue (Askenase et al., 2015). Our data suggest that the sensitivity of monocytes to distal priming by systemic cytokines may be regulated by cell-intrinsic mechanisms controlling the encryption and de-encryption of TF on myeloid cells, which is known to regulate their ability to generate cell surface thrombin and other coagulation proteases (Chen and Hogg, 2013).

ABCA1 is a major regulator of cellular cholesterol and phospholipid homeostasis (Singaraja et al., 2002). It has a key role in atherosclerosis, mediating the efflux of cholesterol and phospholipids and thus reducing the atherosclerotic plaque burden (Pradel et al., 2009). Our data are consistent with other reports that ABCA1 is linked to an anti-inflammatory M2 phenotype (Pradel et al., 2009) and augment the report from Raghavan et al., which first revealed that thrombin downregulates ABCA1 expression (Raghavan et al., 2018) via cullin 3 expression, which is a component of cullin-RING E3 ubiquitin ligase complex involved in protein ubiquitination (Dubiel et al., 2018). ABCA1 has been shown to disrupt cholesterol-rich microdomains via redistribution of cholesterol from rafts to non-rafts through its ATPase-related functions (Zhu et al., 2010). In our study, we were able to show a direct link between thrombin stimulation, ABCA1 down regulation, increase in lipid-rich microdomains at the cell membrane, and increased sensitivity to IFN γ , which, along with the secretion of picomolar concentrations of IFN γ , was the basis for the increased sensitivity to LPS. This is consistent with previous reports that human monocytes when cultured with IFN γ have heightened responses to bacterial LPS (Hayes and Zoon, 1993).

In summary, we have provided the first evidence that thrombin mediated PAR-1 signaling on the surface of monocytes, leading to ABCA1 downregulation and an associated sensitivity to IFN γ , and TLR stimulation is critically involved in the development of normal DTH responses *in vivo*. Targeting this pathway could potentially offer a way to modulate innate immune responsiveness and to control inflammatory responses in multiple diseases.

Limitations of the study

A potential limitation of this work is that we have not confirmed results in mice-deficient in PAR, particularly PAR-1. Our rationale is that both the priming/sensitization and re-challenge phases would be influenced by the lack of PAR-1 signaling. Our approach instead relied upon using highly specific agonists and antagonists to allow us to isolate only the re-challenge phase for study.

We have also not addressed the role of PAR-2 signaling in this model, as our ongoing experiments dissecting the impact of PAR-2 stimulation suggest complex interactions between PAR-2 and PAR-1 stimulation which require further interrogation and will be the subject of a subsequent report. Others have reported that PAR-2 signaling in contact dermatitis contributes to the inflammatory response (Seeliger et al., 2003).

Resource availability

Lead contact

Further information and requests for resources should be directed to and will be fulfilled by the Lead Contact, Hannah Wilkinson (hannah.wilkinson@kcl.ac.uk).

Material availability

This study did not generate new unique reagents.

Data and code availability

This study did not generate data sets or codes.

Methods

All methods can be found in the accompanying [Transparent methods supplemental file](#).

Supplemental information

Supplemental information can be found online at <https://doi.org/10.1016/j.isci.2020.101981>.

Acknowledgments

Support for this work was received through an MRC research training fellow grant MR/P018513/1.

Author contributions

H.W. designed and performed all the experiments and wrote the manuscript. A.D. designed the experiments, supervised the overall project, and assisted in manuscript preparation. H.L. assisted with *in vitro* experimentation. P.G. provided guidance in lipid raft staining techniques. M.R., T.L., and D.C. assisted in experimental design and manuscript review. J.M. assisted in data review and manuscript writing.

Declaration of interests

The authors declare no competing interests.

Received: July 1, 2020

Revised: November 13, 2020

Accepted: December 17, 2020

Published: January 22, 2021

References

- Adamson, S., and Leitinger, N. (2011). Phenotypic modulation of macrophages in response to plaque lipids. *Curr. Opin. Lipidol.* 22, 335–342.
- Antoniak, S., Tatsumi, K., Bode, M., Vanja, S., Williams, J.C., and Mackman, N. (2017). Protease-activated receptor 1 enhances poly I:C induction of the antiviral response in macrophages and mice. *J. Innate Immun.* 9, 181–192.
- Askenase, M.H., Han, S.J., Byrd, A.L., Morais Da Fonseca, D., Bouladoux, N., Wilhelm, C., Konkol, J.E., Hand, T.W., Lacerda-Queiroz, N., Su, X.Z., et al. (2015). Bone-marrow-resident NK cells prime monocytes for regulatory function during infection. *Immunity* 42, 1130–1142.
- Black, C.A. (1999). Delayed type hypersensitivity: current theories with an historic perspective. *Dermatol. Online J.* 5, 7.
- Camerer, E., Gjernes, E., Wiiger, M., Pringle, S., and Prydz, H. (2000). Binding of factor VIIa to tissue factor on keratinocytes induces gene expression. *J. Biol. Chem.* 275, 6580–6585.
- Chen, C.B., Abe, R., Pan, R.Y., Wang, C.W., Hung, S.I., Tsai, Y.G., and Chung, W.H. (2019). Erratum to “an updated review of the molecular mechanisms in drug hypersensitivity”. *J. Immunol. Res.* 2019, 2489429.

- Chen, D., Abrahams, J.M., Smith, L.M., Mcvey, J.H., Lechler, R.I., and Dorling, A. (2008a). Regenerative repair after endoluminal injury in mice with specific antagonism of protease activated receptors on CD34+ vascular progenitors. *Blood* 111, 4155–4164.
- Chen, D., Carpenter, A., Abrahams, J., Chambers, R.C., Lechler, R.I., Mcvey, J.H., and Dorling, A. (2008b). Protease-activated receptor 1 activation is necessary for monocyte chemoattractant protein 1-dependent leukocyte recruitment in vivo. *J. Exp. Med.* 205, 1739–1746.
- Chen, D., Giannopoulos, K., Shiels, P.G., Webster, Z., Mcvey, J.H., Kemball-Cook, G., Tuddenham, E., Moore, M., Lechler, R., and Dorling, A. (2004a). Inhibition of intravascular thrombosis in murine endotoxemia by targeted expression of hirudin and tissue factor pathway inhibitor analogs to activated endothelium. *Blood* 104, 1344–1349.
- Chen, D., Li, K., Festenstein, S., Karegji, J., Wilkinson, H., Leonard, H., Wei, L.L., Ma, N., Xia, M., Tam, H., et al. (2020). Regression of atherosclerosis in ApoE^{-/-} mice via modulation of monocyte recruitment and phenotype, induced by weekly dosing of a novel "cytotoxic" anti-thrombin without prolonged anticoagulation. *J. Am. Heart Assoc.* 9, e014811.
- Chen, D., Weber, M., Lechler, R., and Dorling, A. (2006). NK-cell-dependent acute xenograft rejection in the mouse heart-to-rat model. *Xenotransplantation* 13, 408–414.
- Chen, D., Weber, M., Mcvey, J.H., Kemball-Cook, G., Tuddenham, E.G., Lechler, R.I., and Dorling, A. (2004b). Complete inhibition of acute humoral rejection using regulated expression of membrane-tethered anticoagulants on xenograft endothelium. *Am. J. Transpl.* 4, 1958–1963.
- Chen, V.M., and Hogg, P.J. (2013). Encryption and decryption of tissue factor. *J. Thromb. Haemost.* 11 (Suppl 1), 277–284.
- Chinetti-Gbaguidi, G., Colin, S., and Staels, B. (2015). Macrophage subsets in atherosclerosis. *Nat. Rev. Cardiol.* 12, 10–17.
- Coughlin, S.R. (2005). Protease-activated receptors in hemostasis, thrombosis and vascular biology. *J. Thromb. Haemost.* 3, 1800–1814.
- Cunningham, M.A., Rondeau, E., Chen, X., Coughlin, S.R., Holdsworth, S.R., and Tipping, P.G. (2000). Protease-activated receptor 1 mediates thrombin-dependent, cell-mediated renal inflammation in crescentic glomerulonephritis. *J. Exp. Med.* 191, 455–462.
- Dubiel, W., Dubiel, D., Wolf, D.A., and Naumann, M. (2018). Cullin 3-based ubiquitin ligases as master regulators of mammalian cell differentiation. *Trends Biochem. Sci.* 43, 95–107.
- Favari, E., Zanotti, I., Zimetti, F., Ronda, N., Bernini, F., and Rothblat, G.H. (2004). Probucol inhibits ABCA1-mediated cellular lipid efflux. *Arterioscler Thromb. Vasc. Biol.* 24, 2345–2350.
- Hayes, M.P., and Zoon, K.C. (1993). Priming of human monocytes for enhanced lipopolysaccharide responses: expression of alpha interferon, interferon regulatory factors, and tumor necrosis factor. *Infect. Immun.* 61, 3222–3227.
- Kang, K.W., Choi, S.Y., Cho, M.K., Lee, C.H., and Kim, S.G. (2003). Thrombin induces nitric-oxide synthase via Galpha12/13-coupled protein kinase C-dependent I-kappaBalpha phosphorylation and JNK-mediated I-kappaBalpha degradation. *J. Biol. Chem.* 278, 17368–17378.
- Karegji, J., Melchionna, T., Farrar, C.A., Greenlaw, R., Smolarek, D., Horsfield, C., Charif, R., Mcvey, J.H., Dorling, A., Sacks, S.H., and Smith, R.A. (2017). Thrombalexins: cell-localized inhibition of thrombin and its effects in a model of high-risk renal transplantation. *Am. J. Transpl.* 17, 272–280.
- Leifer, C.A., and Medvedev, A.E. (2016). Molecular mechanisms of regulation of Toll-like receptor signaling. *J. Leukoc. Biol.* 100, 927–941.
- Lopez-Zambrano, M., Rodriguez-Montesinos, J., Crespo-Avilan, G.E., Munoz-Vega, M., and Preissner, K.T. (2020). Thrombin promotes macrophage polarization into M1-like phenotype to induce inflammatory responses. *Thromb. Haemost.* 120, 658–670.
- Manabe, Y., Kono, S., Tanaka, T., Narai, H., and Omori, N. (2009). High blood pressure in acute ischemic stroke and clinical outcome. *Neurol. Int.* 1, e1.
- Manook, M., Kwun, J., Burghuber, C., Samy, K., Mulvihill, M., Yoon, J., Xu, H., Macdonald, A.L., Freischlag, K., and Curfman, V. (2017). Thrombalexin: use of a cytotoxic anticoagulant to reduce thrombotic microangiopathy in a highly sensitized model of kidney transplantation. *Am. J. Transplant.* 17, 2055–2064.
- Mills, C.D. (2015). Anatomy of a discovery: m1 and m2 macrophages. *Front. Immunol.* 6, 212.
- Moore, K.J., Sheedy, F.J., and Fisher, E.A. (2013). Macrophages in atherosclerosis: a dynamic balance. *Nat. Rev. Immunol.* 13, 709–721.
- O'Brien, P.J., Prevost, N., Molino, M., Hollinger, M.K., Woolkalis, M.J., Woulfe, D.S., and Brass, L.F. (2000). Thrombin responses in human endothelial cells. Contributions from receptors other than PAR1 include the transactivation of PAR2 by thrombin-cleaved PAR1. *J. Biol. Chem.* 275, 13502–13509.
- Ostrowska, E., Sokolova, E., and Reiser, G. (2007). PAR-2 activation and LPS synergistically enhance inflammatory signaling in airway epithelial cells by raising PAR expression level and interleukin-8 release. *Am. J. Physiol. Lung Cell Mol. Physiol.* 293, L1208–L1218.
- Pike, L.J. (2003). Lipid rafts: bringing order to chaos. *J. Lipid Res.* 44, 655–667.
- Pradel, L.C., Mitchell, A.J., Zarubica, A., Dufort, L., Chasson, L., Naquet, P., Broccardo, C., and Chimini, G. (2009). ATP-binding cassette transporter hallmarks tissue macrophages and modulates cytokine-triggered polarization programs. *Eur. J. Immunol.* 39, 2270–2280.
- Raghavan, S., Singh, N.K., Mani, A.M., and Rao, G.N. (2018). Protease-activated receptor 1 inhibits cholesterol efflux and promotes atherogenesis via cullin 3-mediated degradation of the ABCA1 transporter. *J. Biol. Chem.* 293, 10574–10589.
- Rao, L.V., and Pendurthi, U.R. (2012). Regulation of tissue factor coagulant activity on cell surfaces. *J. Thromb. Haemost.* 10, 2242–2253.
- Saeed, M.A., Ng, G.Z., Dabritz, J., Wagner, J., Judd, L., Han, J.X., Dhar, P., Kirkwood, C.D., and Sutton, P. (2017). Protease-activated receptor 1 plays a proinflammatory role in colitis by promoting Th17-related immunity. *Inflamm. Bowel Dis.* 23, 593–602.
- Seeliger, S., Derian, C.K., Vergnolle, N., Bunnett, N.W., Nawroth, R., Schmelz, M., Von Der Weid, P.Y., Buddenkotte, J., Sunderkotter, C., Metz, D., et al. (2003). Proinflammatory role of proteinase-activated receptor-2 in humans and mice during cutaneous inflammation in vivo. *FASEB J.* 17, 1871–1885.
- Shrivastava, S., Ma, L., Tham El, L., J, H.M., Chen, D., and Dorling, A. (2013). Protease-activated receptor-2 signalling by tissue factor on dendritic cells suppresses antigen-specific CD4+ T-cell priming. *Immunology* 139, 219–226.
- Singaraja, R.R., Fievet, C., Castro, G., James, E.R., Hennuyer, N., Clee, S.M., Bissada, N., Choy, J.C., Fruchart, J.C., Mcmanus, B.M., et al. (2002). Increased ABCA1 activity protects against atherosclerosis. *J. Clin. Invest.* 110, 35–42.
- Vu, T.K., Hung, D.T., Wheaton, V.I., and Coughlin, S.R. (1991). Molecular cloning of a functional thrombin receptor reveals a novel proteolytic mechanism of receptor activation. *Cell* 64, 1057–1068.
- Xu, W.F., Andersen, H., Whitmore, T.E., Presnell, S.R., Yee, D.P., Ching, A., Gilbert, T., Davie, E.W., and Foster, D.C. (1998). Cloning and characterization of human protease-activated receptor 4. *Proc. Natl. Acad. Sci. U S A* 95, 6642–6646.
- Zhao, P., Metcalf, M., and Bunnett, N.W. (2014). Biased signaling of protease-activated receptors. *Front. Endocrinol. (Lausanne)* 5, 67.
- Zhu, X., Owen, J.S., Wilson, M.D., Li, H., Griffiths, G.L., Thomas, M.J., Hiltbold, E.M., Fessler, M.B., and Parks, J.S. (2010). Macrophage ABCA1 reduces MyD88-dependent Toll-like receptor trafficking to lipid rafts by reduction of lipid raft cholesterol. *J. Lipid Res.* 51, 3196–3206.

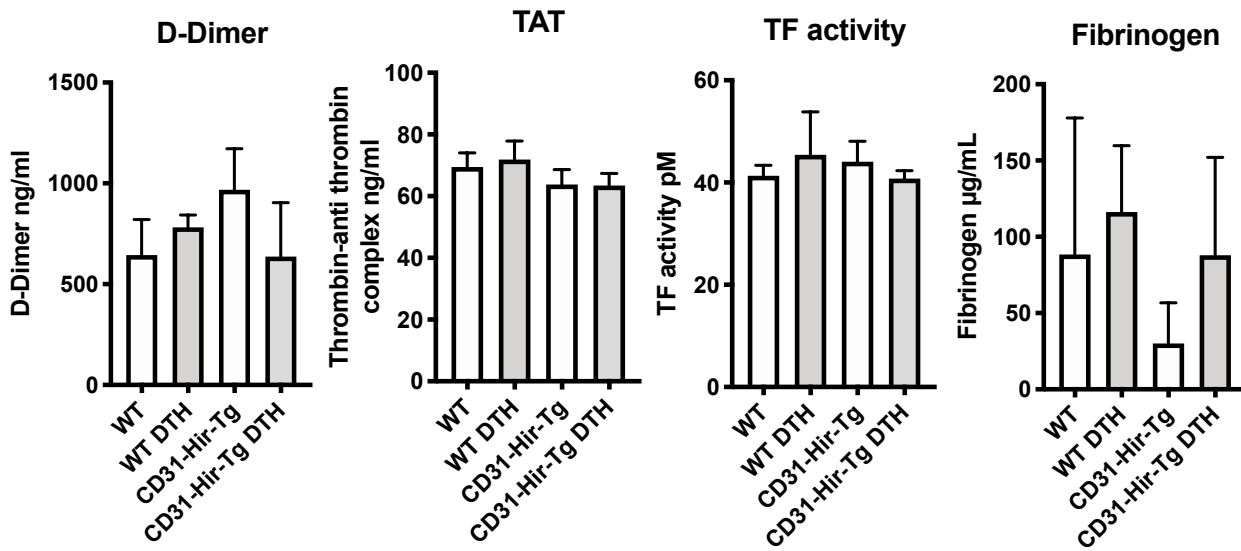
iScience, Volume 24

Supplemental Information

**PAR-1 signaling on macrophages is required
for effective in vivo delayed-type
hypersensitivity responses**

**Hannah Wilkinson, Hugh Leonard, Daxin Chen, Toby Lawrence, Michael Robson, Pieter.
Goossens, John H. McVey, and Anthony Dorling**

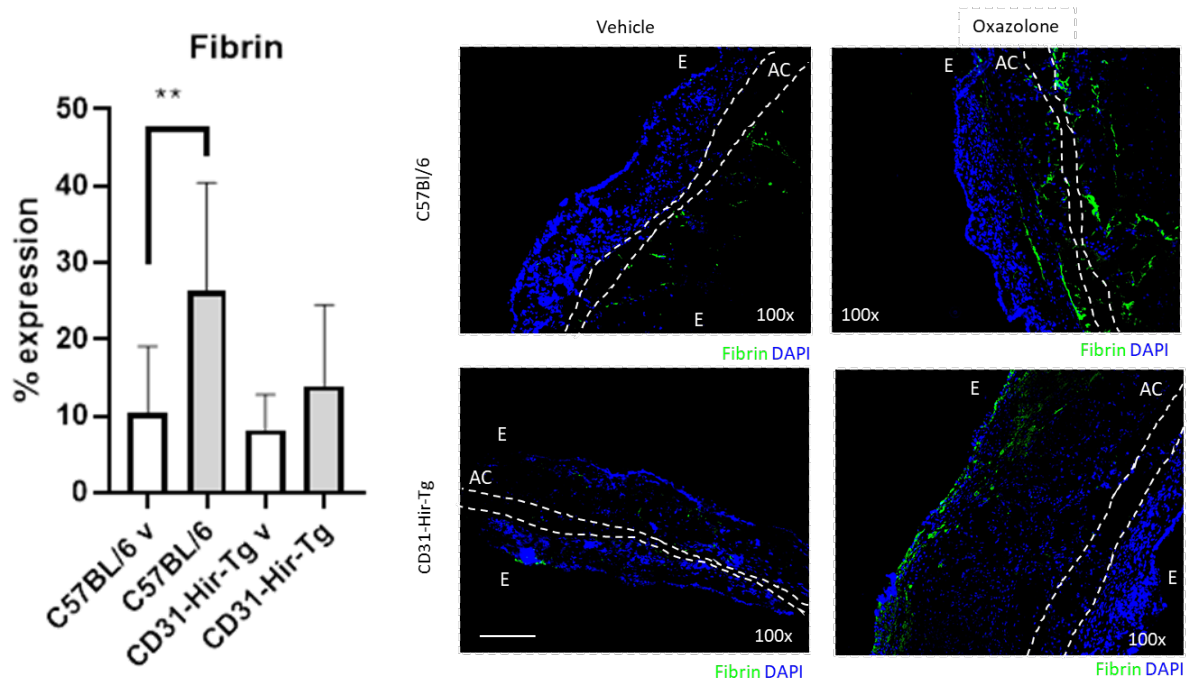
Supplemental Figure 1.



Supplemental Figure 1. Parameters of coagulation in Tg and WT mice. Related to Figure 1.

Plasma TF activity was measured using an activity assay commercially available from Abcam. Plasma D-Dimer, fibrinogen and TAT complex were measured by ELISA in CD31-Hir-Tg and WT mice at baseline and after delayed type hypersensitivity (designated WT DTH or CD31-Hir-Tg DTH). Data are represented as mean \pm SEM.

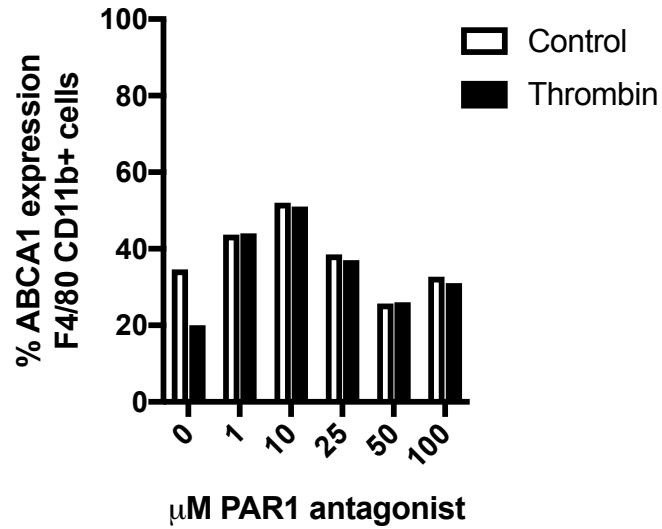
Supplemental Figure 2.



Supplemental figure 2. Fibrin expression in the ears of WT or CD31-Hir-Tg mice after DTH. Related to Figure 1.

Immunofluorescence analysis with associated graphical representation, of Fibrin in the oxazolone and vehicle (v) treated ears of CD31-Hir-Tg and WT mice. Expression calculated by % ear area occupied by Fibrin. Images are representative and show Fibrin (green) with DAPI (blue) E= epidermis, AC= auricular cartilage. Data are represented as mean ± SEM. The scale bar shows 200 μm in distance.

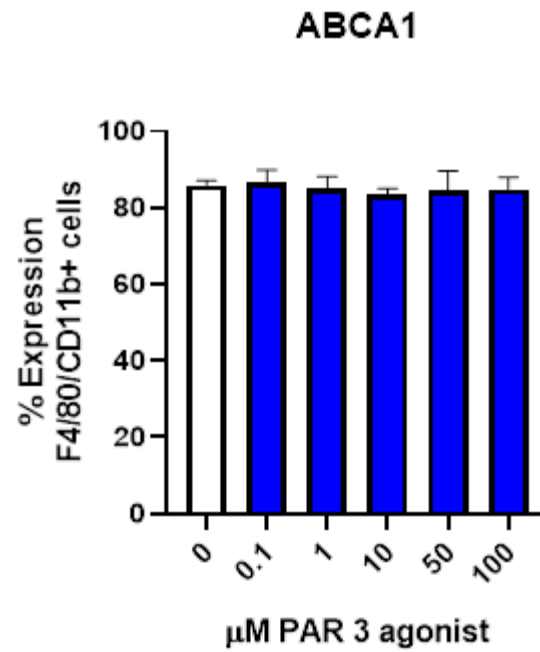
Supplemental Figure 3.



Supplemental Figure 3. ABCA1 expression in response to PAR-1 antagonists. Related to Figure 3G.

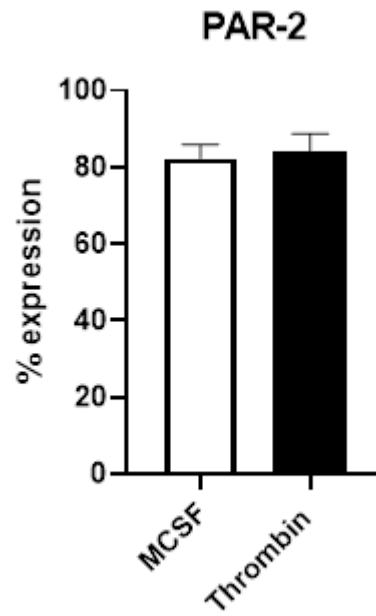
BMM were incubated with increasing amounts of PAR-1 antagonist (FLLRN) for 1 hour prior to the addition of thrombin for a further 23 hours. Control cells were maintained in the PAR-1 antagonist throughout the 24 hours assay. Cells were then analysed for surface ABCA1 expression by flow cytometry. Data are represented as mean \pm SEM.

Supplemental Figure 4.



Supplemental Figure 4. ABCA1 expression in response to PAR-1 antagonists. Related to Figure 3G. ABCA1 expression, analysed by flow cytometry, on F4/80 CD11b positive cells after 5 days in bone marrow culture followed by 24 hours stimulation with 25ng/ml MCSF, thrombin, or increasing amounts of H-Ser-Phe-Asn-Gly-Gly-Pro-NH₂ (PAR3 Tethered Ligand) Data are represented as mean \pm SEM.

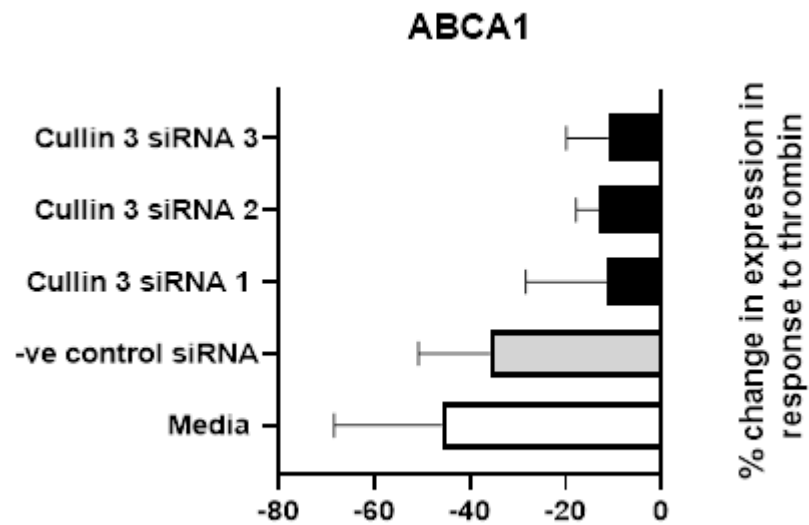
Supplemental Figure 5.



Supplemental Figure 5. PAR-2 expression in response to thrombin stimulation. Related to Figure 3.

Surface PAR-2 expression analysed by flow cytometry on BMM after 24 hours stimulation with 50 units/ml of thrombin or maintained in control media with MCSF. Data are represented as mean \pm SEM.

Supplementary Figure 6.



Supplementary Figure 6. Optimization of Cullin 3 siRNA. Related to Figure 6.

Three siRNAs to cullin 3 were purchased from Thermofischer scientific. (ID siRNA 1-188654; siRNA 2-72389; siRNA3-188655). Cells were transfected for 24 hours prior to thrombin stimulation. Cells were then analysed by flow cytometry for ABCA1 expression. Cullin 3 siRNA # 1 was used in the main data section. Data are represented as mean \pm SEM.

Transparent Methods

Animals: 6-12 week old male C57BL/6 mice were purchased from Envigo and housed in specific pathogen free environment. CD45.1 and CD31-Hir-Tg (Chen et al., 2004) mice were bred in house on a C57BL/6 background. All procedures were performed in accordance with the Home Office Animals (Scientific Procedures) Act of 1986.

Delayed type hypersensitivity experiments: On Day 0 a 50 μ l preparation of 5% oxazolone (Sigma, Dorset, UK) in ethanol and acetone (4:1) was applied to the shaved abdomen. Mice were re-challenged on day 5 by applying 1% oxazolone in olive oil and acetone (4:1, 10 μ l) to the right ear and vehicle alone to the left ear. Ear thickness was measured using a digital micrometre using at least 5 measurements and this was subtracted from the mean ear thickness of the vehicle treated ear. After 48 hours the mice were sacrificed by schedule one methods and the ears removed and added to a cryomold and covered in OCT. Samples were stored at -80°C prior to analysis. In vivo mice were treated with IP PAR agonists/antagonists at the molarity described in the experiments prior to rechallenge on day 5. For the PTL060 experiments mice received 10 μ g/g IV Thrombalexin on day 3 and day 5 (3 hours before re-challenge). For the probucol experiments CD31-Hir-Tg mice received 1mg/kg IP probucol (Stratech, Ely, UK) daily on days 2-5. Immediately after last IP injection, the mice were re-challenged with 1% oxazolone in olive oil and acetone (4:1, 10 μ l) to the right ear and vehicle alone to the left ear.

T cell isolation and adoptive transfer: Mice were sensitised with oxazolone to the shaved abdomen as described above. After 5 days they were culled by a schedule 1 method and their spleens were removed and placed over a 70micron filter. The tissue was disrupted with a plunger and the filter was flushed with 15mls cold DMEM. Red cells were lysed by incubation with ammonium chloride lysis buffer and CD4 cells were isolated using CD4 MicroBeads (Miltenyi Biotech, Woking, UK) as per manufacturer's instruction. 5x10⁶ purified CD4⁺ cells were then injected via the tail vein into naïve recipient WT mice, which were then challenged with 1% oxazolone in olive oil and ethanol to the right ear and vehicle alone to the left. ES was measured at 24 and 48 hours.

Bone marrow transplant: Recipient mice were irradiated with 9 Gy and then reconstituted with 5x10⁶ bone marrow cells (see below for isolation protocol) intravenously via tail vein within 24 hours of irradiation. Mice were weighed daily and monitored for signs of distress. Engraftment was assessed by surface CD45.1 and CD45.2 expression on peripheral blood cells acquired through tail vein venepuncture by flow cytometry after day 30.

Immunofluorescence analysis: Tissue sections were cut (5 μ m) using a cryostat (Bright Instrument Ltd, Huntington, UK) and transferred onto multispot glass slides (Hendley-Essex, Loughton, UK). Sections were fixed in methanol for 1 hour at -20°C and then left to air dry. Sections were then blocked with 10% foetal calf serum (FCS) in PBS for 1 hour after which they were washed 3 times for 5 minutes in PBS 0.5% Triton X-100. Primary antibodies used in this study were rat anti mouse CD68 (FA-11 Thermofischer Scientific, UK) and CD3 (ab5690 Abcam, Cambridge, UK) and rabbit anti mouse CD206 (ab64693 Abcam), iNOS (ab15323 Abcam), ABCA1 (ab7360 Abcam), IL-10 (ab34843 Abcam) and IFN γ (ab9657 Abcam). Primary antibodies were incubated overnight in a humidified chamber, before washing and application of the secondary antibody (goat anti-rat AF594 or goat anti-rabbit AF488 (Abcam)) for 2 hours at room temperature (RT). Slides were mounted with Vectashield Antifade Mounting Media with DAPI (2BScientific, Oxford, UK) and covered with glass cover slips. All sections were stored in the dark at 4 °C before analysis using a fluorescence microscope. For quantification, images were assessed at 100X magnification, background signal was assessed with isotype and no primary controls. Using ImageJ software, the area of the lesion was drawn around and percentage expression assessed using threshold measurements to remove background signal. At least 5 images were taken per section. Colocalisation analysis was performed using Pearson correlation analysis on ICY software.

Bone marrow isolation protocol: Bone marrow cell suspensions were isolated by flushing femurs and tibias of 8-12 week-old donor mice with Dulbecco's Modified Eagle Medium (DMEM). Aggregates were dislodged by gentle pipetting, and debris was removed by passing the suspension through a 70- μ m cell strainer. Isolated cells were counted and plated on a Nunc™ Non-Treated 6 well plate (Thermofischer Scientific) at 1x10⁶ cells/ml in DMEM glutamax, high glucose, high pyruvate (Thermofischer Scientific) supplemented with 10% FCS, 1 % non-essential amino acids, 1% penicillin/streptomycin and 2 μ M Mercaptoethanol (Thermofischer Scientific). To induce macrophage formation 25ng/ml macrophage colony-stimulating factor (MCSF) (Biolegend, London, UK) was added to the culture medium. Cells were then placed in a humidified incubator at 37°C at 5% CO₂. Media was changed for fresh media every 48 hours and grown for 5 - 7 days.

In vitro macrophage stimulation: Cells were used at 1×10^6 cells per ml in DMEM glutamax, high glucose, high pyruvate (ThermoFischer Scientific) supplemented with 10% FCS, 1% non-essential amino acids, 1% penicillin/streptomycin and $2 \mu\text{M}$ Mercaptoethanol, plated in 12 or 24 well plates. For titration experiments cells were exposed to increasing concentrations of LPS or IFN γ . For full M1 polarisation cells were stimulated with 100ng/ml LPS (from *Escherichia coli* O55:B5-Sigma) and 50ng/ml IFN γ (ThermoFischer Scientific), whereas canonical M2 polarisation was achieved by 25ng/ml IL-4 (BD Biosciences, Berkshire, UK). In some experiments, cells were primed with various concentrations of thrombin (Enzyme Research Lab, Swansea UK) for 24 hours prior to exposure to IFN γ , LPS or IL-4. In some experiments, thrombin primed cells were incubated for 1 hour with anti IFN γ (ab9657 Abcam) prior to LPS stimulation. To assess the role of EPCR signalling cells were incubated for 2 hours with a neutralising ePCR antibody CD201 (EPCR) Monoclonal Antibody (eBio1560 (1560) ThermoFischer Scientific) prior to thrombin stimulation. All experiments occurred in 10% FCS containing media.

ELISA: IFN γ and IL-10 ELISA Kits were purchased from ThermoFischer Scientific. Cell culture supernatants, reagents and standards were prepared as per manufacturer's instructions. Plates were read using a *SpectraMax® Plus 384* Microplate Reader (Molecular Devices) using 450nm as the primary wavelength and 620nm as reference wavelength. Data was analysed using *SoftMax® Pro* Software (Molecular Devices) and Excel software (Microsoft).

Flow Cytometry: All flow cytometry was performed on a Fortessa LSR II flow cytometer (Becton Dickinson) using DIVA software (Becton Dickinson) and analysed using Flow-jo (Treestar, Ashland, OR) software. Prior to surface staining cells were incubated with mouse Fc Block (Biolegend) for 5 minutes in the dark at 4°C, after which 50 μL of the relevant antibody cocktail was added, and the cells were left to incubate in the dark at 4°C for 30 minutes. Surface antibodies were FITC – F4/80, APC- CD11b, PE-ABCA1 (Santa Cruz Biotechnology, Heidelberg, Germany). After surface staining cells were resuspended in 200 μl pre-diluted Near IR live/dead stain (Life Technologies) and left to incubate in the dark at 4°C for 15 minutes. For intracellular staining, cells were permeabilised with Foxp3 intracellular staining permeabilisation solution for 30 minutes (e-Bioscience). Intracellular staining was performed using directly conjugated antibodies (BV605-CD206 (Biolegend) and PE-Cy7-iNOS (e-Bioscience)) made up into a staining cocktail using permeabilisation buffer (e-Bioscience), 50 μL of staining cocktail was added per well and staining took place at 21 °C in the dark.

Lipid raft staining: Lipid rafts were stained using Vybrant™ Alexa Fluor™ 488 Lipid Raft Labeling Kit from ThermoFischer scientific. Cells were plated on 8-well borosilicate IF wells (Nunc LabTek) at 1×10^5 cells/well in 200 μl DMEM. 50U/ml Thrombin or MCSF was added to the wells and the cells were left overnight in an incubator at 37°C at 5% CO $_2$. The following day, after two washes with cold, serum-free DMEM, cells were incubated with 200 μl CT-B-Alexa488 (1:1000 in serum-free DMEM for 10 minutes in the dark at 4°C. Following further washes with IF buffer containing PBS + 5% FCS + 10mM glycine, cells were incubated at RT for 2 hours with 500 μl of 1:200 Rabbit α CT-B in serum free DMEM. For co-staining the primary antibody (Anti-TLR4 (ab13867) or IFN- γ R β Antibody (Santa Cruz)) was added to the Rabbit anti-CT-B for the first hour, the wells were then washed and for the second hour the secondary (goat anti-rabbit AF594 or goat anti-hamster AF594 (ThermoFischer scientific)) was added to the Rabbit anti-CT-B. After a final washing step with IF buffer cells were fixed with 4% paraformaldehyde (PFA) for 10 minutes. Nuclear staining was undertaken with DAPI. Images were acquired using Image using an inverted confocal microscope @ 60x magnification (oil immersion) and analyzed using NIS-Elements software.

SiRNA: BMM were plated at 2×10^5 cells/ml in DMEM 10% FCS. 500 μL cell suspension was added to a 24 well plate. SiRNA was prepared using Lipofectamine™ RNAiMAX Transfection Reagent with Opti-MEM™ Reduced Serum Medium and Silencer™ Pre-Designed siRNA (ThermoFisher Scientific). Cells were transfected in complete medium for 24 hours as per manufacturers instruction at 37°C at 5% CO $_2$. FITC conjugated positive control siRNA and negative control siRNA was also used (sc-36869 and sc-37007 respectively, Santa Cruz). After 24 hours 50U/ml thrombin was added, and cells were further incubated for 24 hours at 37°C at 5% CO $_2$. After this 24-hour incubation the cells were then washed and new media with LPS/IFN γ with or without thrombin was added for a further 24 hours. Cells were then analysed for ABCA1 and iNOS expression using flow cytometry as described above.

Western blot: Cells were removed from the tissue culture plate with 150 μL RIPA buffer (Abcam). Protein quantification was performed using the Pierce™ BCA Protein Assay Kit (Thermo Scientific). The XCell Surelock™ Mini-Cell (Invitrogen, California) was set up using pre-cast gels 4-12% (Biorad) and PageRuler™ Plus Pre stained Protein Ladder (ThermoFisher) was used as control. The gel was set to run at 200v for 35 minutes. The XCell II blot module (Invitrogen, California) was used to transfer proteins from

the gel to a nitrocellulose membrane (Biorad) The transfer was run for 1 hour at 30v. The membrane was blocked for 1 hour in 5% powdered milk w/v (Marvel, UK) in TBS + 0.1% Tween-20 (TBST). Primary antibody Anti-ABCA1 antibody (ab7360) (Abcam) was added at 1/500 and anti-rabbit GAPDH (1/10000) in 5% milk in TBST overnight at 4°C. The secondary antibody (Anti Rb IRDye® 800CW, Li-Cor) was added at 1:10000 in TBST with 1% BSA for 1 hour at room temperature. Images were acquired using Odyssey® Fc Imaging System and analysed using Image Studio Lite (both Li-cor).

RT PCR: RNA was extracted using RNeasy mini Kit (Qiagen). RNA quantity was analysed by Nano drop system. Reverse transcription was carried out using the QuantiTect Reverse transcription Kit (Qiagen). Genomic DNA was eliminated using the provided gDNA wipe-out buffer. The PCR step was performed using TaqMan fast advanced master mix with TaqMan gene expression assays (ThermoFisher scientific). PCR assays used were: TBP (Mm01277042_m1), iNOS (Mm00440502_m1), TNF α (Mm00443258_m1), IL-1 β (Mm00434228_m1), IL-6 (Mm00446190_m1) and RANTES (Mm01302427_m1). The plate was then set up on the BioRad CFX96 Real Time PCR detection system. The results were then compared to the housekeeping gene TATA box binding protein (TBP).

Statistical analysis: All statistical analyses were performed using GraphPad Prism® software version 7. Unpaired samples were compared using a Mann Whitney U test with two tailed p-values. P-values are shown as *P \leq 0.05, ** P \leq 0.01, ***P \leq 0.001, **** P \leq 0.0001.

Supplemental references

CHEN, D., GIANNOPOULOS, K., SHIELS, P. G., WEBSTER, Z., MCVEY, J. H., KEMBALL-COOK, G., TUDDENHAM, E., MOORE, M., LECHLER, R. & DORLING, A. 2004. Inhibition of intravascular thrombosis in murine endotoxemia by targeted expression of hirudin and tissue factor pathway inhibitor analogs to activated endothelium. *Blood*, 104, 1344-9.